AD 429031

DEFENSE DOCUMENTATION CENTER

FOR

SCIENTIFIC AND TECHNICAL INFORMATION

CAMERON STATION, ALEXANDRIA, VIRGINIA

LPC Report No. 609-P-8

DESIGN, FABRICATION AND HYDROTESTING
OF A 120-INCH DIAMETER PRESSURE VESSEL
USING 18 PERCENT NICKEL
MARAGING STEEL

to

AIR FORCE FLIGHT TEST CENTER
Edwards Air Force Base, California

Research Contract Status Report No. 8

Contract No. AF 04(611)-8525

Period Covered:
10 October to 12 November 1963

25 November 1963

Prepared by: Approved by:

L. Colbert   *J. W. Buffington*
L. Colbert   J. W. Buffington
Project Engineer   Assistant Program Manager
                                                Large Solid Motors

LOCKHEED PROPULSION COMPANY
P. O. Box 111
Redlands, California

LOCKHEED PROPULSION COMPANY

CONTRACT ACTIVITY AND PROGRESS

The significant events which occurred during this report period, 10 October
to 12 November 1963, are listed below.

(1) The Final Report, Metallurgical Analysis of Fractured Closure
     Plate of the 120-inch Maraging Steel Prototype Vessel, by Dr. G.K.
     Bhat of Mellon Institute, was issued. A copy of this report is
     attached.

(2) Repair of the 120-inch diameter vessel proceeded on schedule
     Retest of the repaired vessel is scheduled for mid-December.

UNCLASSIFIED

LPC
609-P-8
22 Nov '63

Lockheed Propulsion Company, P. O. Box 111, Redlands, California. "DESIGN, FABRICATION, AND HYDROTESTING OF A 120-INCH DIAMETER PRESSURE VESSEL USING 18 PERCENT NICKEL MARAGING STEEL." 22 November 1963. Research Contract Status Report No. 8. (1) p. Contract No. AF 04(611)-8525.

UNCLASSIFIED REPORT

The Final Report, "Metallurgical Analysis of Fractured Closure Plate of the 120-inch Maraging Steel Prototype Vessel, by Dr. G. K. Bhat of Mellon Institute, was issued. Repair of the 120-inch diameter vessel proceeded on schedule.

UNCLASSIFIED

METALLURGICAL ANALYSIS OF FRACTURED CLOSURE PLATE

OF THE 120-INCH MARAGING STEEL PROTOTYPE VESSEL

Final Report

by

G. K. Bhat

Submitted to:

Lockheed Propulsion .Company
Redlands, California

Attention: Mr. K. G. Miller
             Material and Subcontracts Manager

             Mr. L. Colbert
             Engineering Division

Under:

LPC P.O. No. 47262-609
Mellon Institute Project 4604

MELLON INSTITUTE
4400 Fifth Avenue
Pittsburgh 13, Pennsylvania

ACKNOWLEDGEMENT

ABSTRACT

~~This report describes~~ the detailed metallurgical analysis work performed in order to determine the cause of closure plate fracture during hydroburst testing of the Lockheed-Excelco 120-inch diameter, maraging 18 per cent nickel steel prototype booster case.

The metallographic and mechanical strength data presented ~~in this report~~ has led to the belief that delamination of the plate welded to the ring forging is largely responsible for the failure of the closure plate at around half the designed membrane stress. The delamination itself seems to have been triggered by the yielding of the retained austenite and cracking of carbides and nitrides in the banded areas of the plate, leading to the formation of a chain of small cracks followed by interplanar separation in the plate.

A second possible cause of closure plate separation is linked with the failure of a large portion of the shear lip in the ring forging. This evidence indicates a design deficiency. However, further confirmation of this second cause must come from the designer of the motor case.

Despite the aforementioned problems, the maraging 18Ni steel of 250 Ksi strength level used in the construction of large diameter booster cases promises to be the best candidate material.

The banding and delamination problems are currently receiving adequate attention from the steel producers and it is expected that solutions will be found in the near future to eliminate or alleviate these undesirable material features.

INTRODUCTION

This report describes the metallurgical analysis work conducted
at Mellon Institute on the fractured closure plate attached to the 120 in.
diameter prototype booster case constructed out of maraging 18 per cent
nickel, 250 Ksi nominal strength level steel.

The closure plate itself was constructed using a machined ring
forging to which a dished plate was welded on. Sixty-eight tapered 1 in.
bolt holes had been drilled in the closure plate ring forging.

Prior to hydroburst testing, the chamber and the test closure were
reportedly subjected to three pressurization cycles. The first one to 600
PSig, the later two to 1500 Psig or an equivalent hoop stress of approxi-
mately 160,000 psi. After the first 1500 Psi pressurization test, all weld
areas had been radiographically inspected and also dye checked. The chamber
and the closure plate were found to be in good condition. The second 1500
Psi pressurization test was performed on June 19, 1963, for the purpose of
conducting a stress-analysis using strain gages. The assembly was at full
1500 Psi pressure for nearly one hour while strain readings were taken. Sub-
sequent to this test the vessel and the closure had been partially inspected
through dye penetrant application. In the areas checked, no indications of
any damage were apparent.

The final hydroburst test was conducted on June 21, 1963. The
chamber, during the interim period from July 19, was standing on the hydro-
test stand over the water sump exposed to the moist and humid environmental
conditions. During the final hydroburst test, at approximately 2000 psi
gage pressure either the test closure bolts failed or the closure plate itself
fractured. Strain readings taken at this pressure, indicated that the case had

sustained hoop stress around 215,000 psi. This stress is roughly 86 per cent of
expected minimum tensile strength of the plate.

At burst, the closure had been forced down through the steel grating
which then hit the concrete pit four feet below. The chamber itself was lying
inclined at an angle as shown in Figure 1. The test stand which was supported
on steel girders had been driven down with such force that the two 26" beams
were badly twisted. The closure plate had broken into several pieces
approximately 65 per cent of the main fracture was through the thicker forging.
The 5/8" plate welded on to the forging had also fractured and delaminated.

On June 27, 1963, the fractured closure plate was reassembled at
Mellon Institute. Personnel representing Mellon Institute, Naval Research
Laboratory, Excelco Developments, Incorporated, and United States Steel Corpor-
ation conducted a preliminary visual examination of the fracture surfaces in
an effort to determine the possible cause of closure plate failure. The broken
parts of the closure plate had been lightly oiled to prevent rusting during
shipment from Excelco to Mellon Institute. This oil had been removed by
spraying carbon tetrachloride on the fracture surfaces and drying the sprayed
area by blowing hot air.

At the conclusion of this preliminary examination failure was attri-
buted to one of the two following possibilities:

(a) A crack which existed in the weld joining the closure plate to
     the ring forging initiated fracture. This crack was not de-
     tected prior to the final hydrotest since a complete inspection
     of the aft closure plate had not been made after the second 1500
     psig pressurization test.

(b) A single bolt or a number of bolts had failed due to stress corrosion
     or lack of adequate notch strength (toughness) or due to the ef-
     fect of the forces developed due to abrupt opening of the crack
     in the weld.

Plate delamination as a possible primary cause of fracture was con-

MELLON INSTITUTE

Figure 1. Showing 120 inch Maraging Steel Vessel Position After Closure
Separation (Picture - Courtesy of Excelco)

sidered but not given much importance. One side of the origin, at the loca-

tion of what was termed as a pre-existent crack in the weld was missing at the

first examination of the fractured closure plate.

Preliminary reports made by all observers had urged a full scale

metallurgical investigation because of the complex appearance of fracture

surfaces seen in the 5/8" thick steel fracture closure plate.

Accordingly, a proposal to this effect was submitted to the cogni-

zant Air Force agency through Lockheed Propulsion Company. Approval of the

technical scope and the necessary funds were obtained during August 1963.

The metallurgical investigation outlined below was then initiated.

The objectives of this program are as follows:

(1) Obtain pictorial records of fracture paths in the top and bottom
     side of the closure plate.

(2) Obtain enlargements of primary and secondary origins of fracture
     i.e. visible defects in the closure plate.

(3) Establish fracture travel directions for determining least re-
     sistant sections for crack propagation.

(4) Characterize fracture textures through light microscopic and
     electron microscopic and electron fractographic examinations
     and associate fractures with inherent parent material and weld
     strength and ductility parameters.

(5) Conduct metallographic studies of laminated sections in an ef-
     fort to develop a method of detecting suspect plates.

(6) Determine the effects of segregation in altering the texture
     of fracture surfaces. This will be studied using metallographic
     and fracture toughness test data.

(7) Determine the stress corrosion susceptibility of bolts by
     torquing the bolts to three levels of load (300 lbs., 600 lbs.,
     1,200 lbs.) and exposing the pretorqued bolts to humid envir-
     onments.

(8) Determine the notched bar and smooth bar tensile properties of
     bolt material.

(9) Determine tensile strength, Charpy impact strength, grain size
and where feasible, bend fracture toughness of material repre-
senting the forging, 5/8" plate, forging-to-plate weldments.

(10) Prepare a detailed final report of above studies.

DETAILED VISUAL AND MACROSCOPIC EXAMINATION

The top and bottom view of the fractured closure plate are as de-
picted in Figures 2 and 3, respectively. Close up views of the various textures
seen in the fractured surfaces in the closure plate, forging and the forging-to-
plate weld are shown in Figures 4, 5, and 6. The nature and extent of delamina-
tion observed in the 5/8" thick plate is as shown in Figure 7.

Figure 3 also indicates the 0.2 wide sliver which came off the shear
lip of the forging.

Figure 8 shows the various fracture travel paths and the direction
of fracture travel in the closure plate. The fracture paths have cut through
the 13th and 40th bolt hole from the reference bolt hole numbered 1. There
were no visible defects in the forging although the fracture path had been
mostly in the forging. The locations from which the metallographic and fracto-
graphic examination specimens were extracted have also been indicated in this
figure. The I beam impact area markings on the closure plate have also been
traced in Figure 8. Fractures close to this area undoubtedly could have re-
sulted from the impact of the closure plate on the I beam.

An examination through a 15X stereoscopic microscope of what has
been termed as a pre-existent crack and probably primary origin in Figure 9
indicated that stained area is actually burnt areas in the weld. An X-ray
diffraction pattern taken on filings from this location indicated presence
of a large amount of Fe_3O_4 and austenite.

The "weld burn markings were spread in the shape of a semi-illip-
tical crack indication. Since the counterpart piece of metal at this location
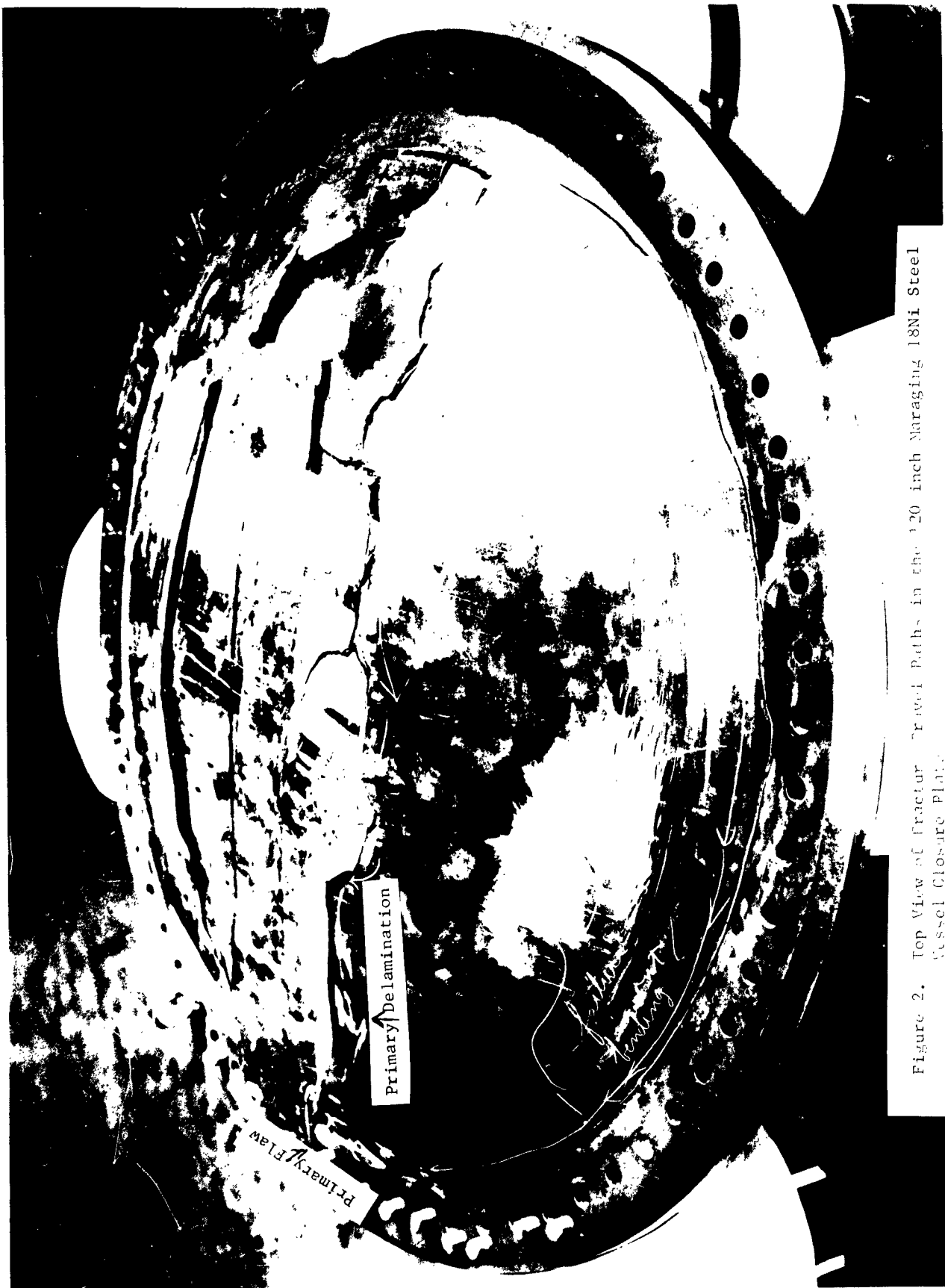
Figure 2. Top View of Fracture Travel Paths in the 120 inch Maraging 18Ni Steel Vessel Closure Plate.
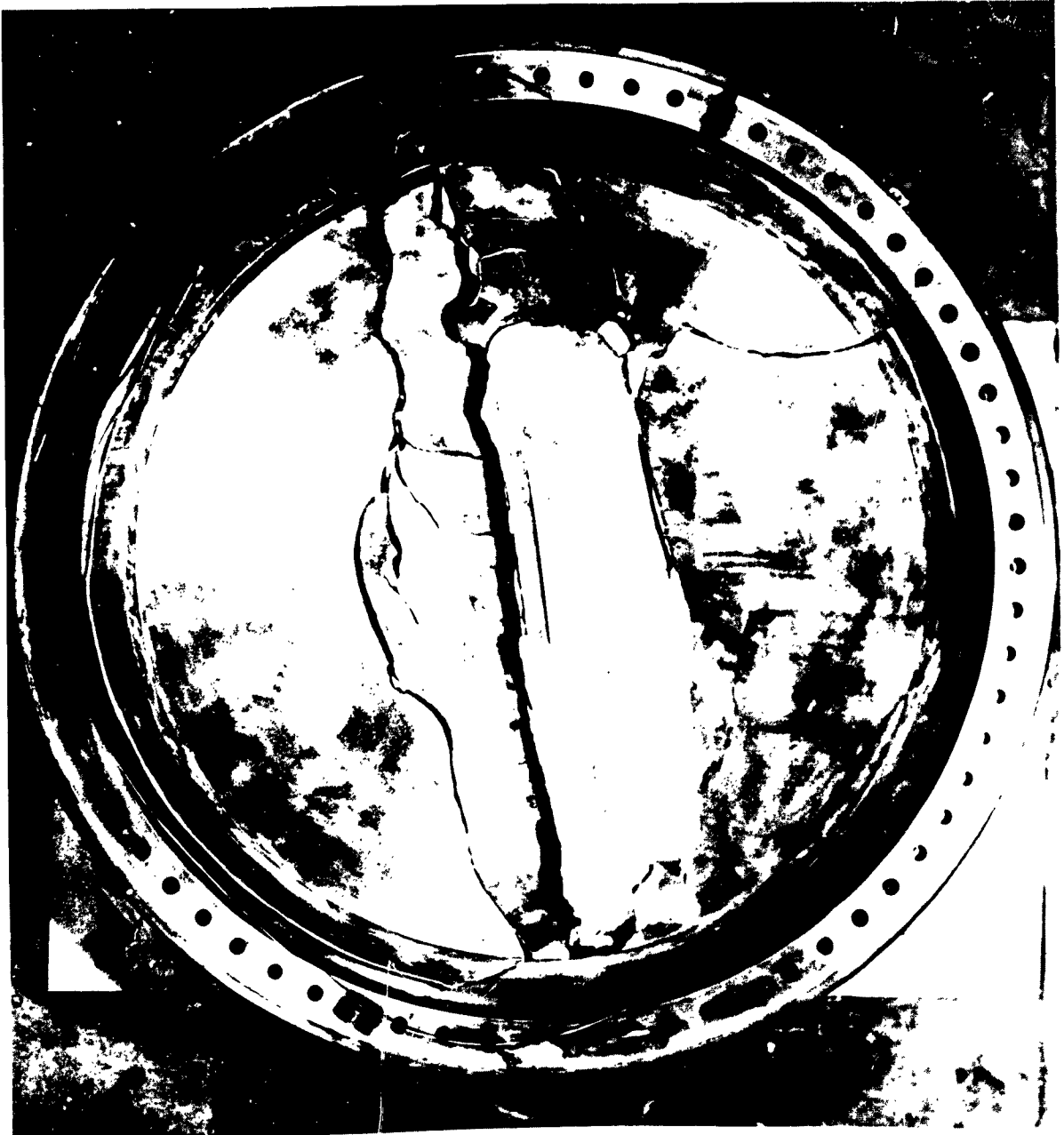
Figure 3. Bottom View of Fracture Travel Paths in the 120 inch Maraging 18Ni Steel Vessel Closure Plate
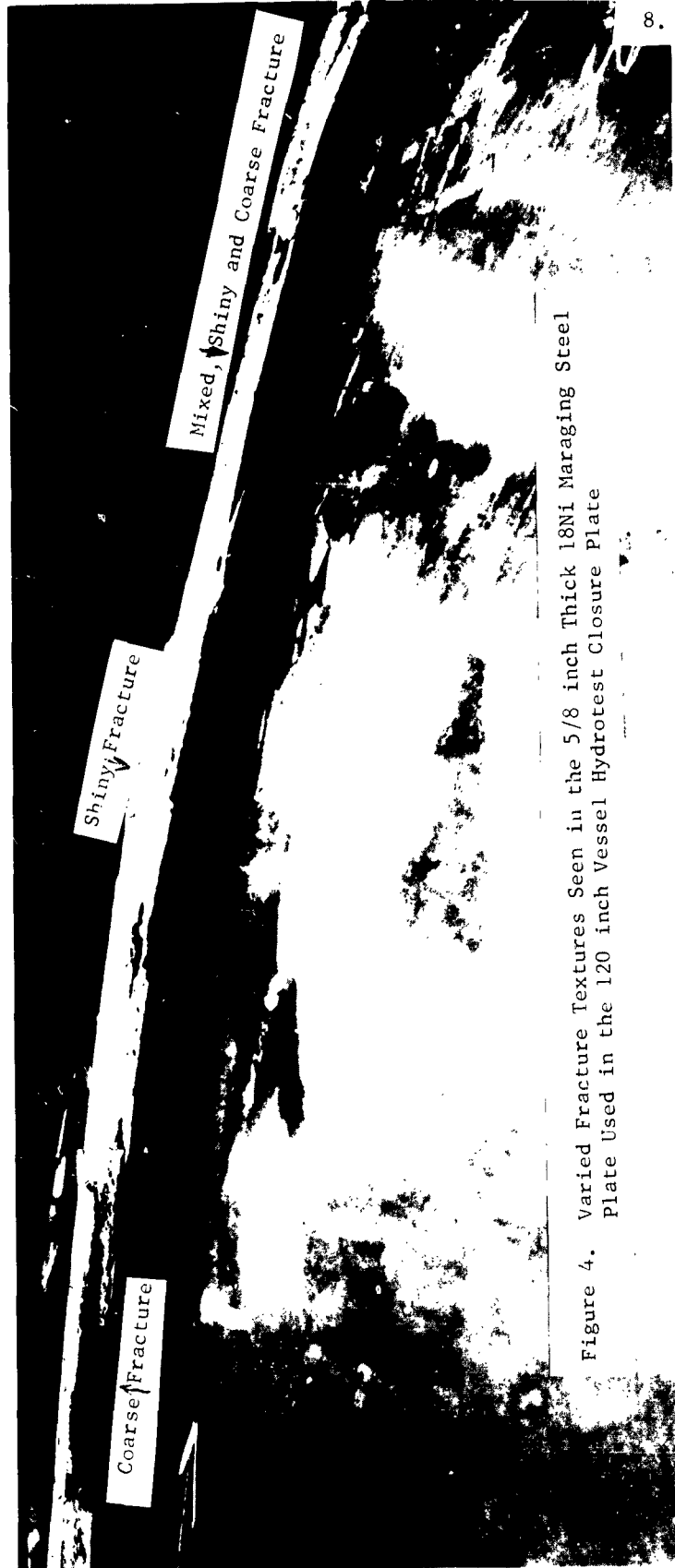
Figure 4. Varied Fracture Textures Seen in the 5/8 inch Thick 18Ni Maraging Steel Plate Used in the 120 inch Vessel Hydrotest Closure Plate

Figure 6. Fracture Surfaces in 120 inch Vessel Closure Plate Ring Forging

Figure 7. Nature and Extent of Delamination Seen at Primary Fracture Origin. Note Also White Bands Indicating Progressive Growth of Delamination Either During Plate Forming or During Hydroburst Test.

Figure 8

BOLT 40

WELD

13 BOLTS
TENSION FAIL

WELD FLAW "F"
1/16 DEEP 3/4 LONG

X-RAY DIFFERENT

EFS = FIG 47-55

MS = FIG 14-19

MS = FIG 36-37

MS = FIG 24-27

MS = FIG 20-22

EFS
NO PICTURES

MS = No PICTURES

BENDING DOWN IND OUT

BENDING DOWN IND OUT

"I" BEAM IMPACT

EMS = FIG 39-46

REFERENCE BOLT 1

BOLT 13

EFS – Electron
Fractographic Spe-
cimens
MS – Metallographic
Specimens
EMS – Electron Micro-
scopic Specimen
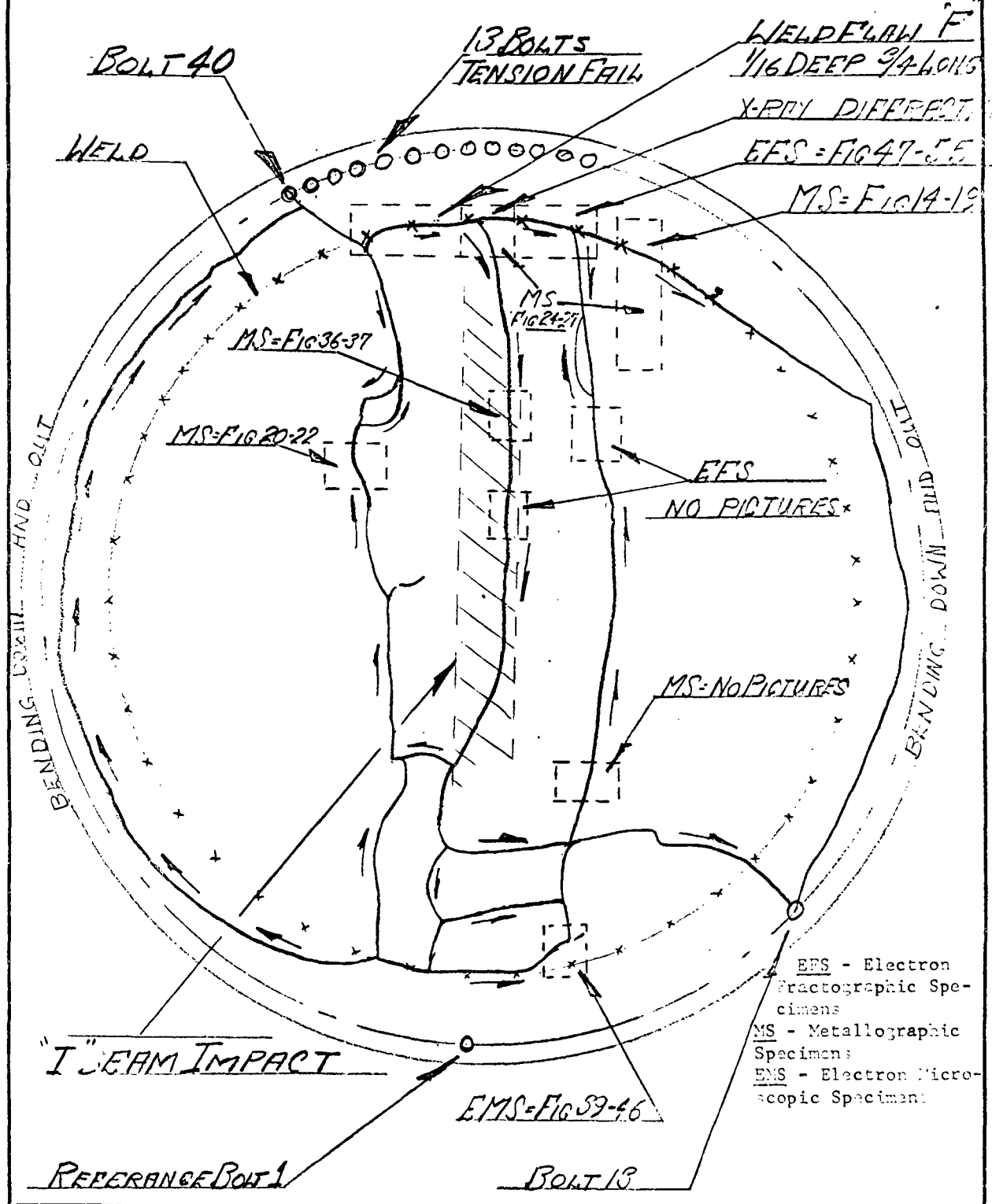
Figure 8	MELLON INSTITUTE, PITTSBURGH, PA.
REVISION	FRACTURE DELINEATION – CLOSURE 120"
REF. DWGS.	DATE 10/28/63 · DRAWN · CHARGE NO.
DWG. NO.	SCALE NONE · CHECKED FRITSCHE · APPROVED

Figure 9. Primary Fracture Origin Where the Delaminated Plate Separated from
the Ring Forging at the Weld. Arrows Indicate Stained Area Mis-
takenly Identified as a Pre-existent Crack.

was missing at the time of the preliminary examination, an error of judgement had obviously resulted. When this metal piece was found, it indicated no evidence of a pre-existent crack. Thus the "crack theory" leading to fracture of the closure plate had to be modified. Physical evidence in support of this decision is shown in Figure 10.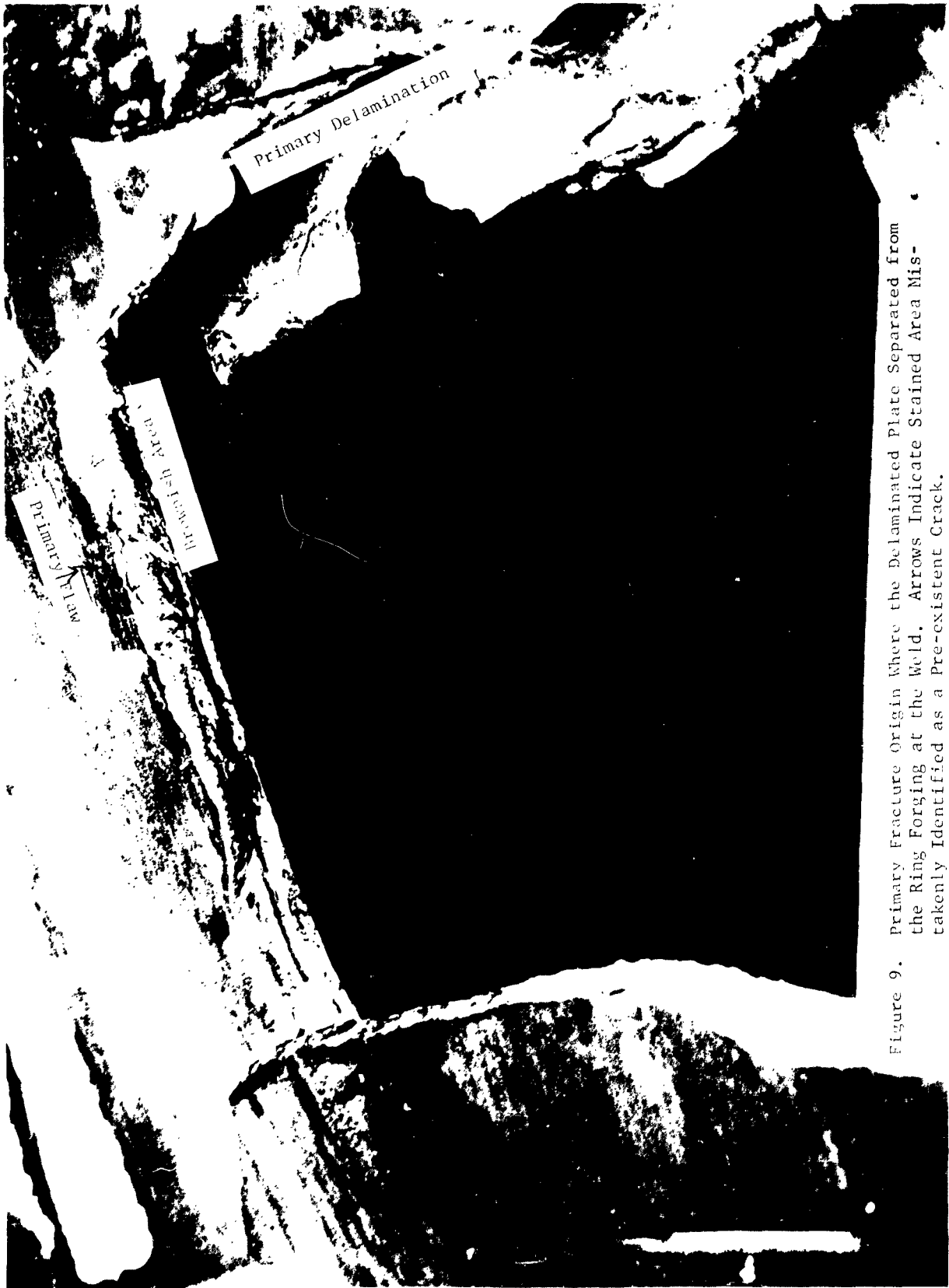 Indeed, when the pieces were put together, in Figure 11, it was evident that considerable yielding had occurred in the closure plate instead of abrupt fracture.

Two secondary origins noted in the closure plate fracture were then thoroughly examined. The pictures of these are presented in Figures 12 and 13. Metallographic evidence indicated large inclusions in these secondary origin locations. It was later concluded that the primary fracture did not originate from these inclusions because the mechanical properties of material in adjacent areas were higher than the minimum expected values.

Metallographic and Fractographic Studies

The next task completed was that of characterization of fracture textures through light microscopic, electron microscopic and electron fracto-graphic examinations.

Specimens for these studies were extracted from areas adjacent to the delaminated sections. A cross-section representing the forging, weld and the 5/8" plate was prepared for metallographic examination and studied under the light microscope. Unetched microstructure at 100X showing general inclusion distribution in the forging are depicted in Figures 14 and 15. In Figures 16 through 19, the austenite and inclusion concentration in typical banded areas are revealed. It is of particular interest here to note the kink in the austenite in Figure 18 and transverse microcracks in the band adjacent to weld heat affected zone in Figure 19.

Figure 10. Mating Fracture Surfaces Indicating No Evidence of Pre-existent Crack At "Primary Origin." (Data refuting "Crack Theory" of Premature Failure of Closure)

Figure 11. Showing Evidence of Yielding in the 5/8 inch Thick Plate Close to the Forging-to-Plate Weld Leading to Delamination of the Plate

Figure 12. One of the Two Secondary Fracture Origin Sites Found in the 120 inch Vessel Closure Plate Forging-to-Plate Weld - Bottom Fractograph Showing Mixed Textures in the Fracture Surface (14X)

MELLON INSTITUTE

Large Inclusion Location
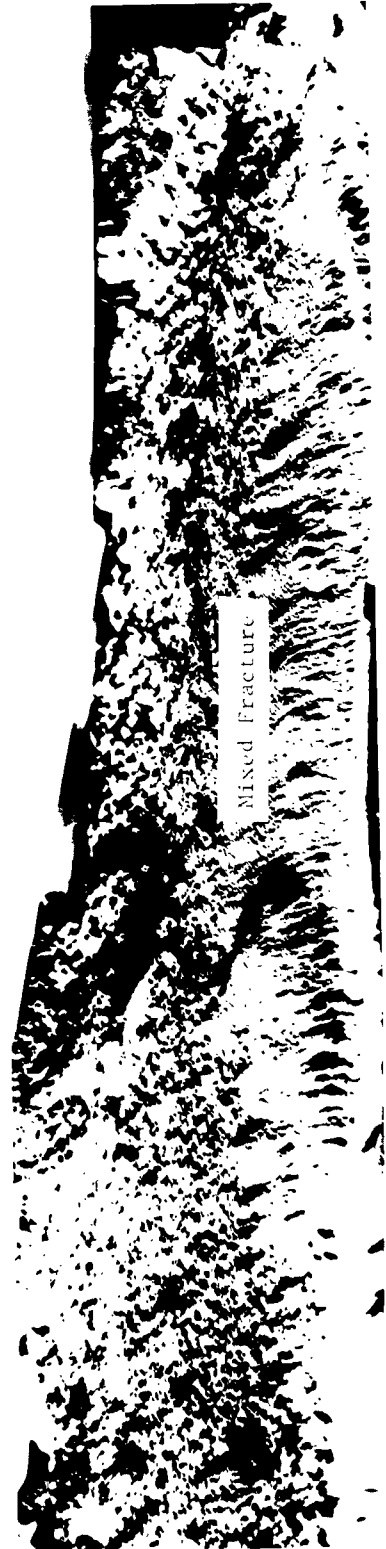
Figure 13. Another of the Two Secondary Fracture Origin Sites Found in the 120 inch Vessel Closure Plate

Figure 14. Inclusion Distribution in the Unaged Material of 120 inch Vessel
Closure Plate Ring Forging

Figure 15. Inclusion Distribution Found in the Maraged 120 inch Vessel Closure
Plate Ring Forging at the Delamination Site
Unetched   100X
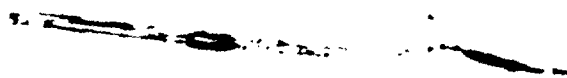
Figure 16. Stringer Type Inclusions and Austenite Patches Found in 5/8 inch
Plate Used in the 120 inch Vessel Closure Plate
Unetched

100X

Figure 17. Stringer Type Inclusions and Austenite Patches Found in 5/8 inch
Plate Used in the 120 inch Vessel Closure Plate
Unetched
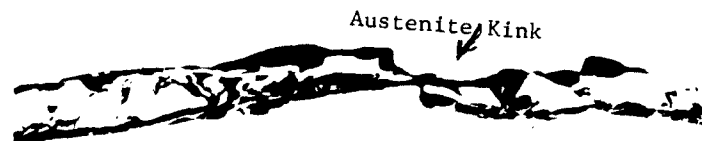
100X

Figure 18. Kinking of the Inclusion or Austenite Band Seen in 5/8 inch Plate
            Close to a Delamination
                        Unetched   100X

Figure 19. Transverse Micro-cracking Seen in the Austenite Band in 5/8 inch Plate
            Close to a Weld
                        Unetched   100X

Figures 20 through 22 show moderately banded areas in the 5/8"
plate. These are alternately dark and light etching bands. Micro-hardness
transverses made through these sections indicated no significant hardness
differential. The appearance of these bands in the weld area is as shown in
Figure 23. Mechanical tests such as, tensile, fracture and bend tests, con-
ducted on material representing this moderately banded condition revealed no
significant degradation. (Data will be found in a later section)

Examples of more severe banding were found in plate close to a
large delamination. These are shown in Figures 24, 25, 26, and 27. The white
area is large amounts of austenite in the band. Microhardness checks revealed
markedly lower hardness as compared to that of fully maraged material. The
weld grains had either inclusions or austenite at almost each grain corner
with large amounts of austenite at termination point of a band at the weld-
parent plate interface.

For comparison purposes, the weld-forging interface microstructures
are presented in Figures 28 through 31. These microstructures are character-
ized by the absence of banding.

First evidence of austenite yielding in the banded areas, prior to
general yielding, was uncovered in heavily delaminated regions of the closure
plate. Figure 32 shows crack formation in a band. Figure 33 shows evidence
of austenite deformation and kink formation and crack development in the in-
clusion line in front of the austenite in the band. Another example of kink
formation leading to cracking is clearly shown in Figure 34. The slippage of
material in a crack leading to widening of the crack which eventually causes
delamination to occur is exhibited in Figure 35.

Specific examples showing that delamination occurs in austenite rich
bands and not in other austenite poor bands are shown in Figures 36 and 37.

MELLON INSTITUTE

Figure 20. Microstructures of Moderately Banded Plate Adjacent
to a Weld   Area A   Chloride Etch   100X

Figure 21. Microstructures of Moderately Banded Plate Adjacent
to a Weld   Area B   Chloride Etch   100X

Figure 22. Microstructures of Moderately Banded Plate Adjacent to a Weld
Area C   Chloride Etch   100X

Figure 23. Weldment - 5/8 inch Plate Interface Microstructure (120 inch Closure
Plate Metallographic Analyses)
Chloride Etch   100X
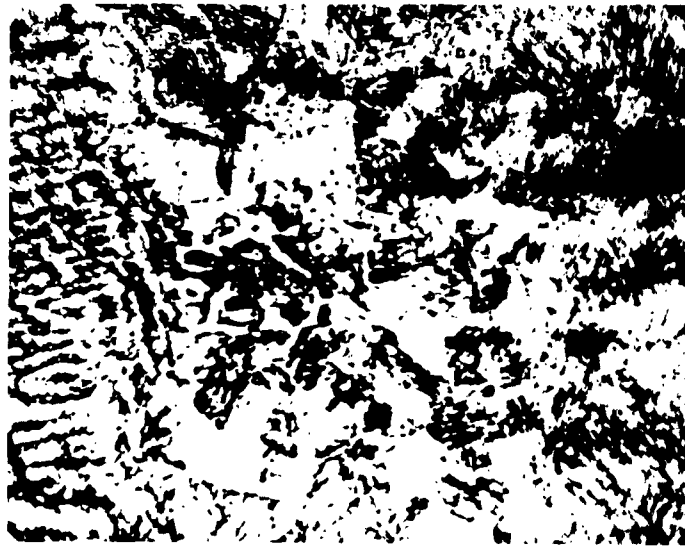
Figure 24. Microstructures Displaying Examples of Severe Banding Which Will Lead
to Delamination of the Plate at the Weld.

MELLON INSTITUTE

Figure 25. Austenite Concentration in Weld Interdendritic Areas

Figure 26. Two Bands of Austenite and Inclusions, and Austenite Concentration in
          Weld Grain Interfaces
                    Chloride Etch   100X

MELLON INSTITUTE

Figure 1. [illegible caption]
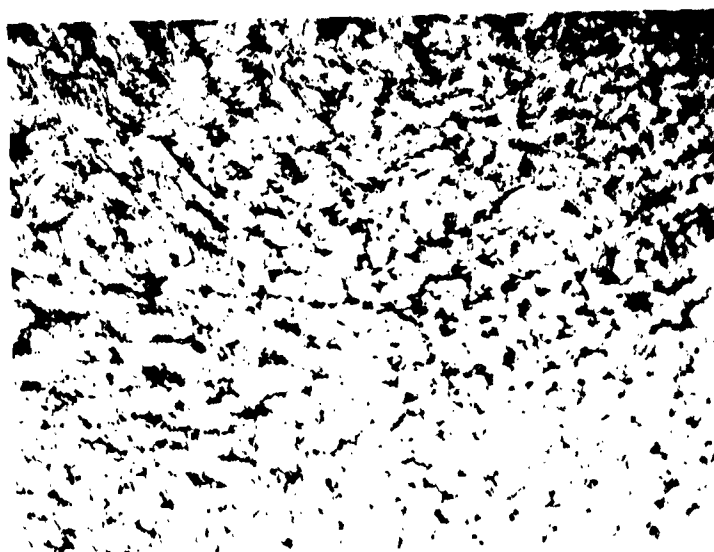
MELLON INSTITUTE

Figure 28. Microstructure of Ring Forging Side of the Weld
Chloride Etch 100X

Figure 29. Microstructure of Weld Center
Chloride Etch 100X
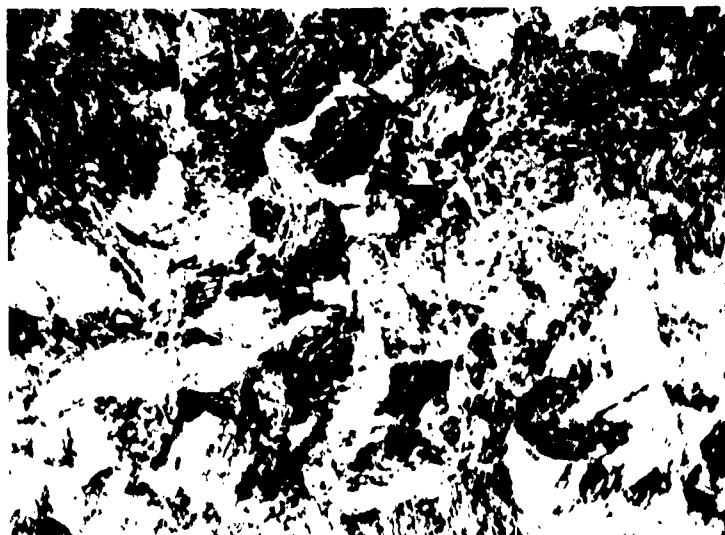
Figure 30.   Microstructure of Weld Fusion Zone - Forging Side
Chloride Etch   100X

Figure 31.   Microstructure of Weld Heat Affected Zone - Forging Side
Chloride Etch   100X
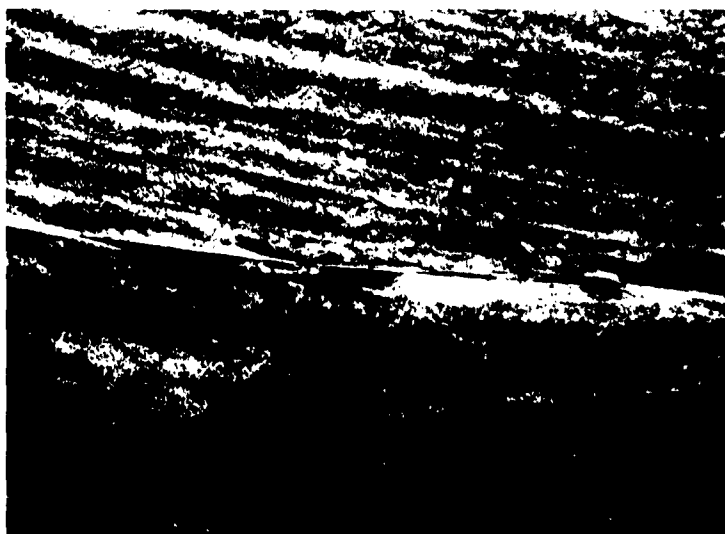
Figure 32. Microstructure Showing Crack Formation in a Deformed Band (5/8 inch
thick Maraging 18Ni (250 Ksi) Plate of 120 inch Vessel Closure Plate)
Chloride Etch   100X

Figure 33. Microstructure Showing Kinking and Crack Formation in a Deformed Band
(5/8 inch Thick Maraging 18Ni (250 Ksi) Plate of 120 inch Vessel
Closure Plate)
Chloride Etch   100X

MELLON INSTITUTE

Figure 34. Microstructures Showing Events Leading to Plate Delamination (Top View) Showing Kinking and Crack Formation in Bands

Figure 35. Top View Showing Material Slippage and Separation at a Delamination (5/8 inch Thick Maraging 18Ni (250 Ksi) Plate of 120 inch Vessel Closure Plate. Specimens Taken at Location P)
Chloride Etch   100X

Figure 36. Microstructure Showing Delamination Occurrence Through Austenite Rich Bands and Not in Other Austenite Poor Bands   Chloride Etch   100X

Figure 37. Microstructure Showing Delamination Occurrence Through Austenite Rich Bands and Not in Other Austenite Poor Bands   Chloride Etch   100X

Electron micrograph showing an austenite rich band in the parent plate material in which fissuring has occurred is shown in Figure 38.

Typical electron microstructures seen in selected areas of the plate to forging weld transition section of the closure plate 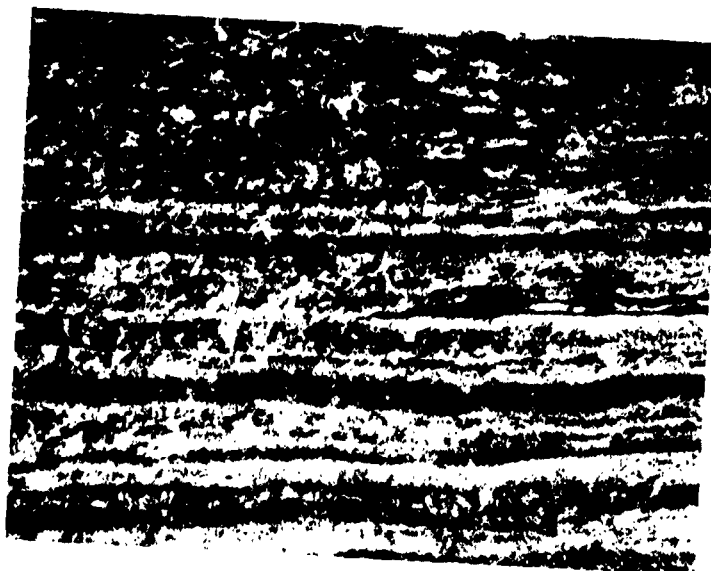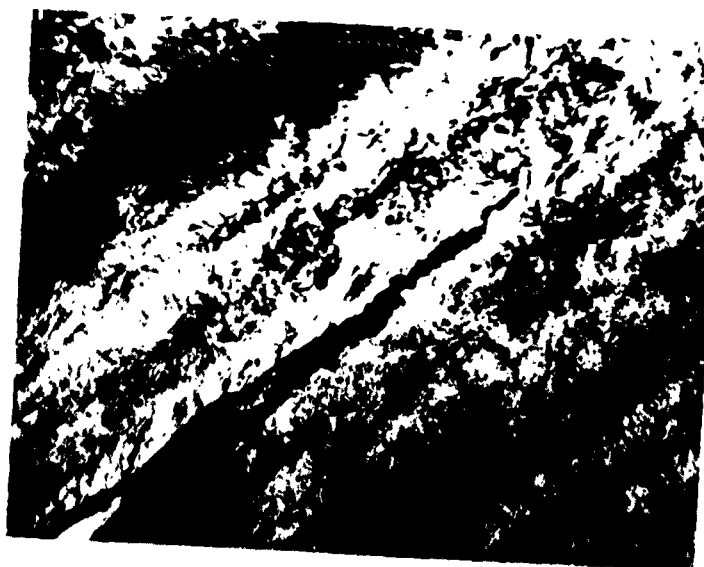are as depicted in Figures 39 through 46. Pertinent explanations of these electron micrographs and identification of the microconstituents observed are given at the bottom of each picture. The complexity of the microstructure in the banded areas is clearly evident. Unique identification of the band microconstituents must await further studies through the use of an electron microprobe analyzer. Interpretation of similar microstructures as provided by earlier investigations, (1, 2)* has been freely used in the preliminary identification of microconstituents in subject electron micrographs.

Since the fracture surface texture appearance differed significantly in various sections of the 5/8" plate, electron fractographic studies were conducted for obtaining a clearer understanding of the fracture mode. Replication techniques used in this study include both single stage, direct carbon method and the two stage, cellulose acetate-carbon method. The latter method is used first and the same sample used for direct carbon replication which leads to the destruction of the fracture surface.

It is pertinent to comment here that some artifacts have occurred during replication. These have been recognized in the interpretation of the fractographs.

Figure 47 shows typical ductile fracture seen in the forging, consisting of nearly elliptical domains. In the light of systematic studies of

---

* 1. Pellissier, G. E., "Some Microstructural Aspects of Maraging (250) Steel in Relation to Strength and Toughness, U. S. Steel Corporation Report
   2. Floreen, S. and Decker, R. F., Trans ASM 55, 1072 (1962)

Figure 38. Electron Micrograph Showing Fissuring in a Deformed Austenite Band -
Specimen from 5/8 inch Thick Plate of 120 inch Vessel Closure Plate
13,000X   Plastic Replica

Figure 39.   Electron Micrograph Showing Micro-cracks in Austenite Adjacent to
              a Weld
                  24,000X   Plastic Replica

Figure 40. Electron Micrographs Showing Inclusions, Voids and Austenite in Weld-
Banded Plate Interface
6,900X   Plastic Replica

Figure 41. Typical Weld Electron Microstructure Seen in Center of Weld Bead, 120 inch Maraging 18Ni Steel Vessel Closure Plate
13,000X   Plastic Replica

Figure 42. Micro-cracking and Staining (Rust Spots) Seen in Maraging Steel
Weldments in Bonded Plates. 120 inch Vessel Closure Plate
Electron Micrograph 13,000X   Plastic Replica

Figure 43. Inclusions, Carbides, Nitrides Seen in Maraging 18Ni, 5/8 inch
Thick Plate Adjacent to a Weld
Electron Micrograph 6,900X   Plastic Replica

Figure 44. Electron Microstructure of Dark Etching Area of the Weld-Plate Interface. 120 inch Vessel Closure Plate Weld
6,900X   Plastic Replica

Figure 45. Typical Electron Microstructure Showing Clam Shell Shaped Titanium Carbides or Nitrides at Forging-Weld Fusion Zone. 120 inch Maraging 18Ni Steel Vessel Closure Plate
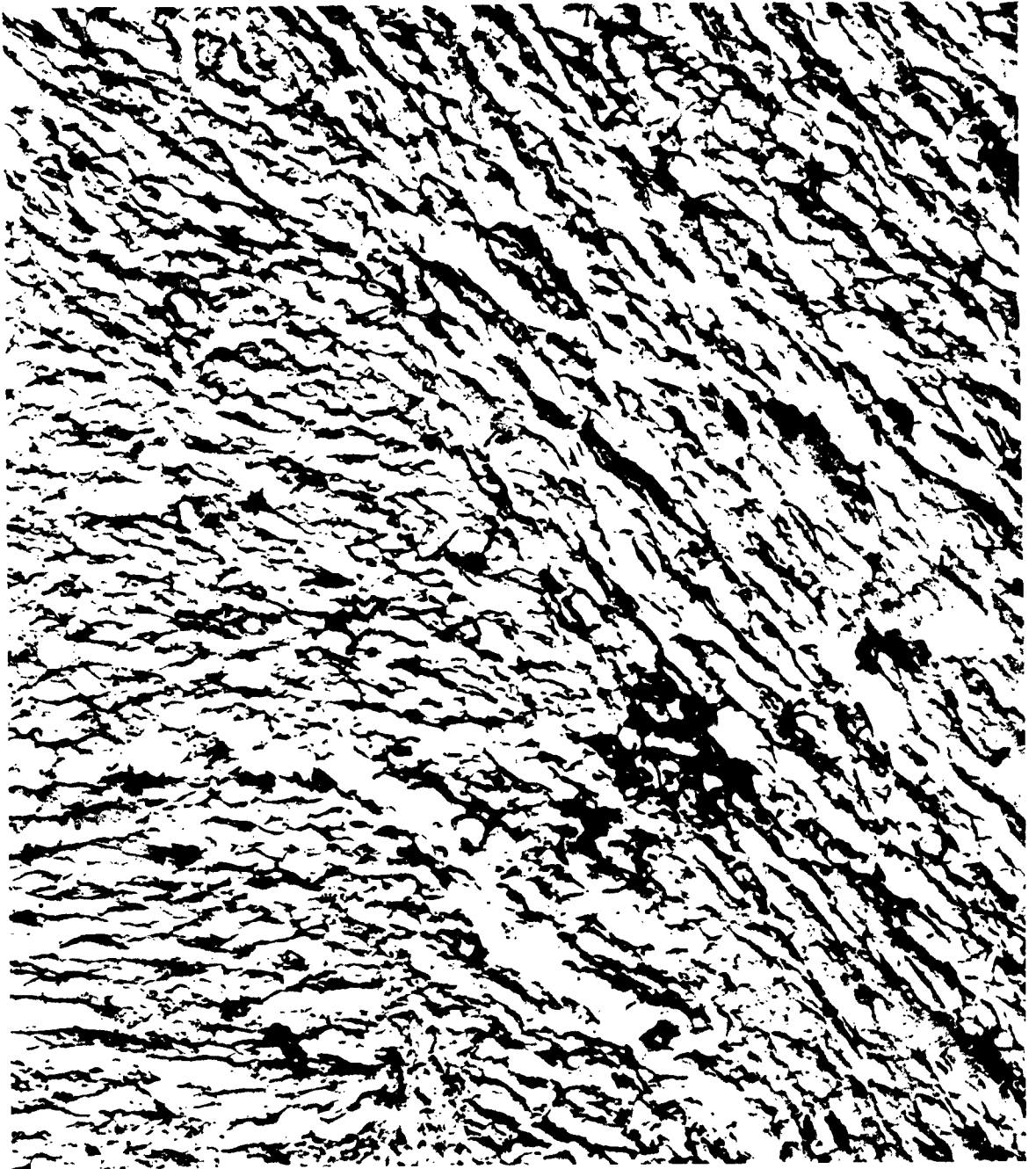24,000X   Plastic Replica

Figure 46. Typical Electron Microstructure of Ring Forging Used in 120 inch
Maraging 18Ni Steel Vessel Closure Plate
13,000X   Plastic Replica
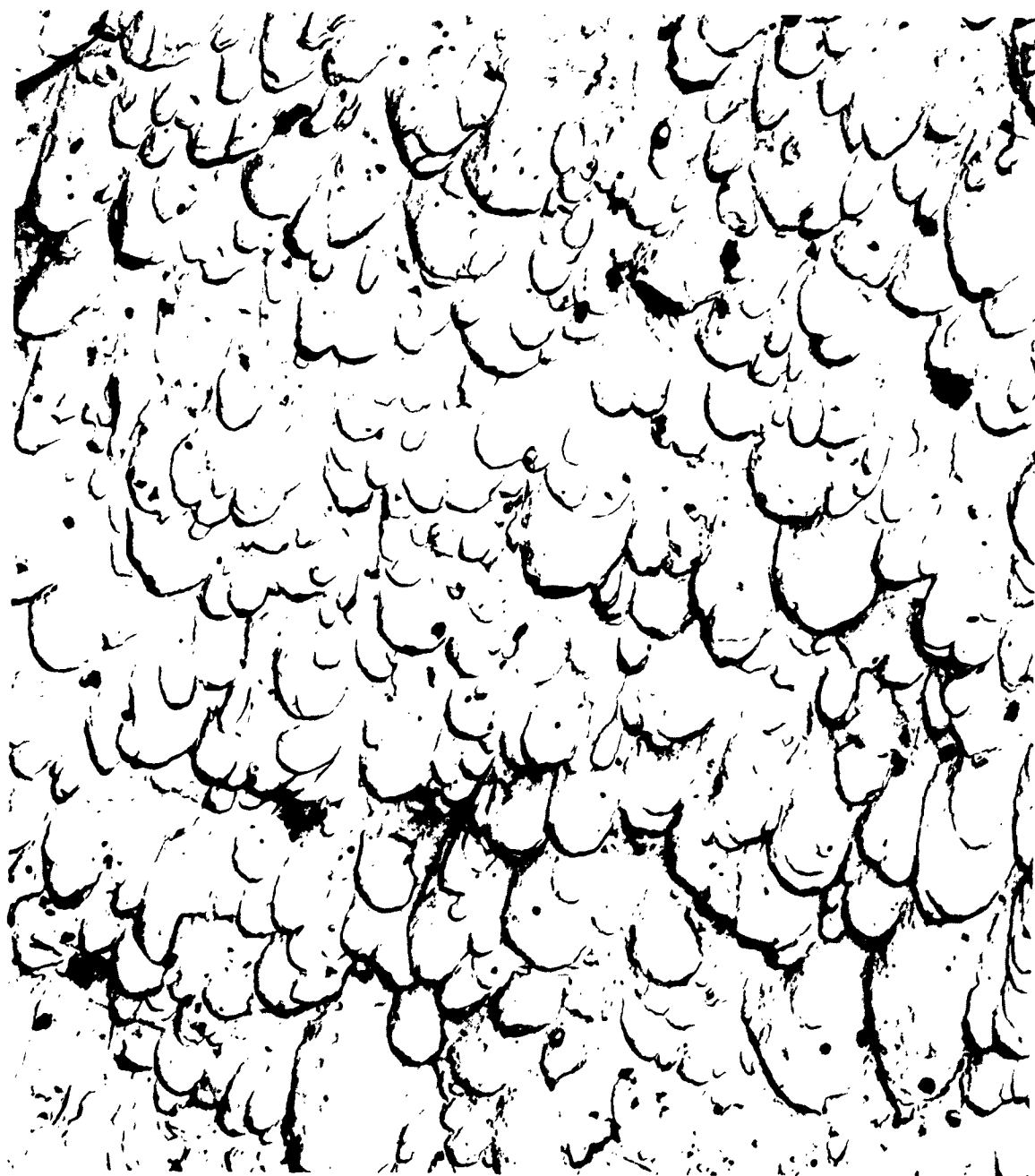
Figure 47. Electron Fractograph Showing Ductile Fracture Surfaces in the Forging
            Consisting of Nearly Elliptical Domains - 120 inch Maraging 18Ni Steel
            Vessel Closure Plate
                  12,000X   Formvar Replica

fracture surfaces conducted by several investigators, it can be inferred that fracture in the closure plate forging has occurred by the formation growth, and union of internal ruptures at inclusions.

Electron fractographs obtained from fracture surface adjacent to the weld joining the plate to the forging (location) indicates severe plastic deformation and long shear lips as indicated in Figure 48. To the naked eye, this surface appears quite shiny and misleading. Except for the electron fractographic evidence, one could argue on this as brittle type fracture. Fracture surface in the weld per se appears as shown in Figure 49. The dark appearing long laths are probably titanium carbo-nitrides or titanium carbides. The welds are replete with respect to these microconstituents.

Fracture appearance of austenite rich bands observed the 5/8 inch plate is as shown in Figure 50. The same picture at 24,000 magnification is shown in Figure 51.

The development of kinks due to localized deformation in the austenite bands can be seen in Figures 52 and 53.

The occurrence of cracks at the termination of deformed austenite bands adjacent to a weld is as indicated in Figure 54.

Interplanar shear leading to formation of folds or steps in which a crack front is developed can be seen in Figure 55.

Since detailed studies for the identification of specific constituents seen in these electron fractographs have not been conducted, no explanations as to the exact mechanism of crack formation and fracture are offered. Nevertheless, the above studies have been rewarding, in that some new light has been shed on the causes of delamination. The tendency for delamination has been definitely associated with the incidence of large amounts of austenite in the banded areas.
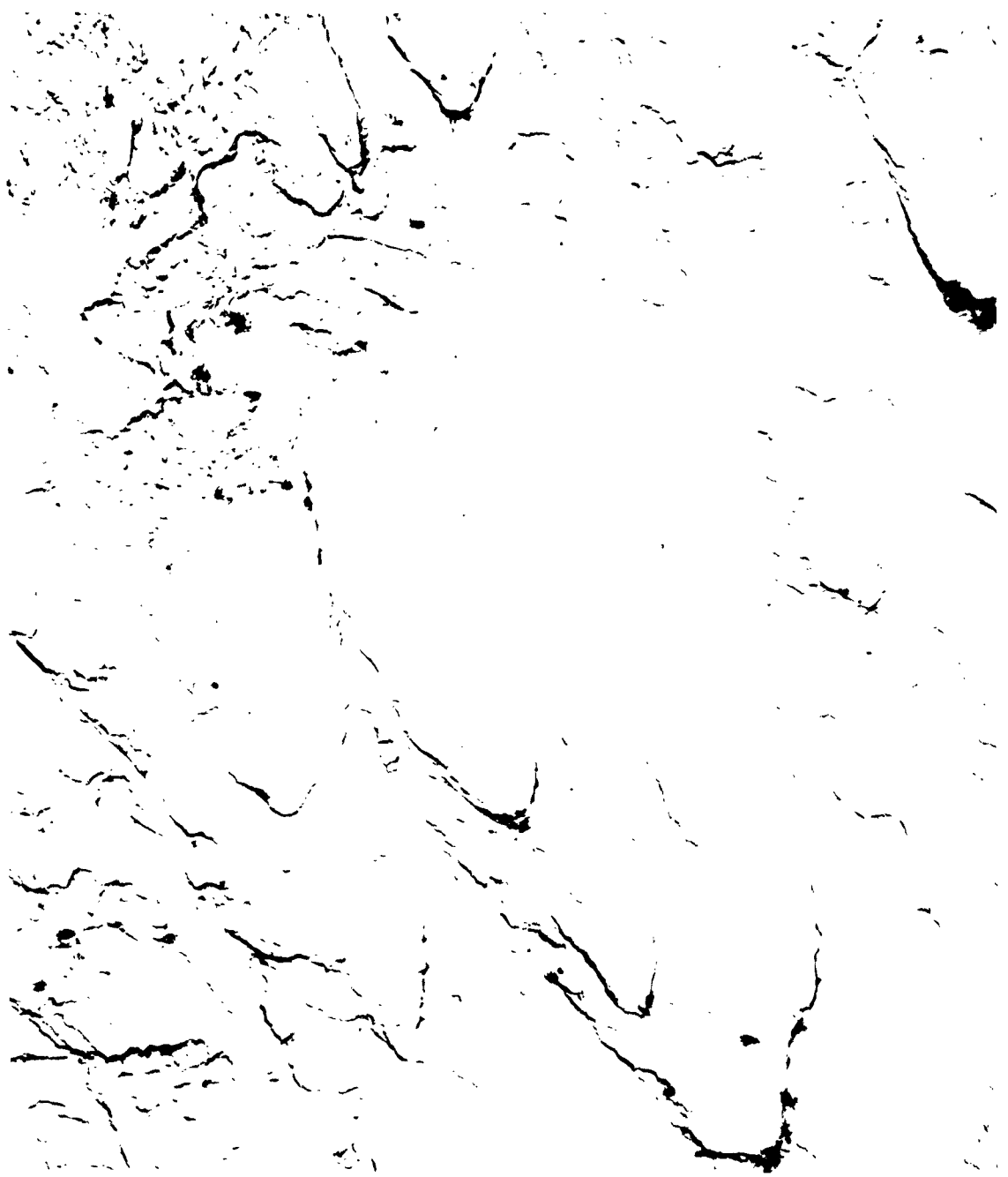
Figure 48. Electron Fractograph of Fracture Surface Adjacent to Weld Joining
the Plate Displaying Severe Plastic Deformation - Long Shear Lips
24,000X   Formvar Replica
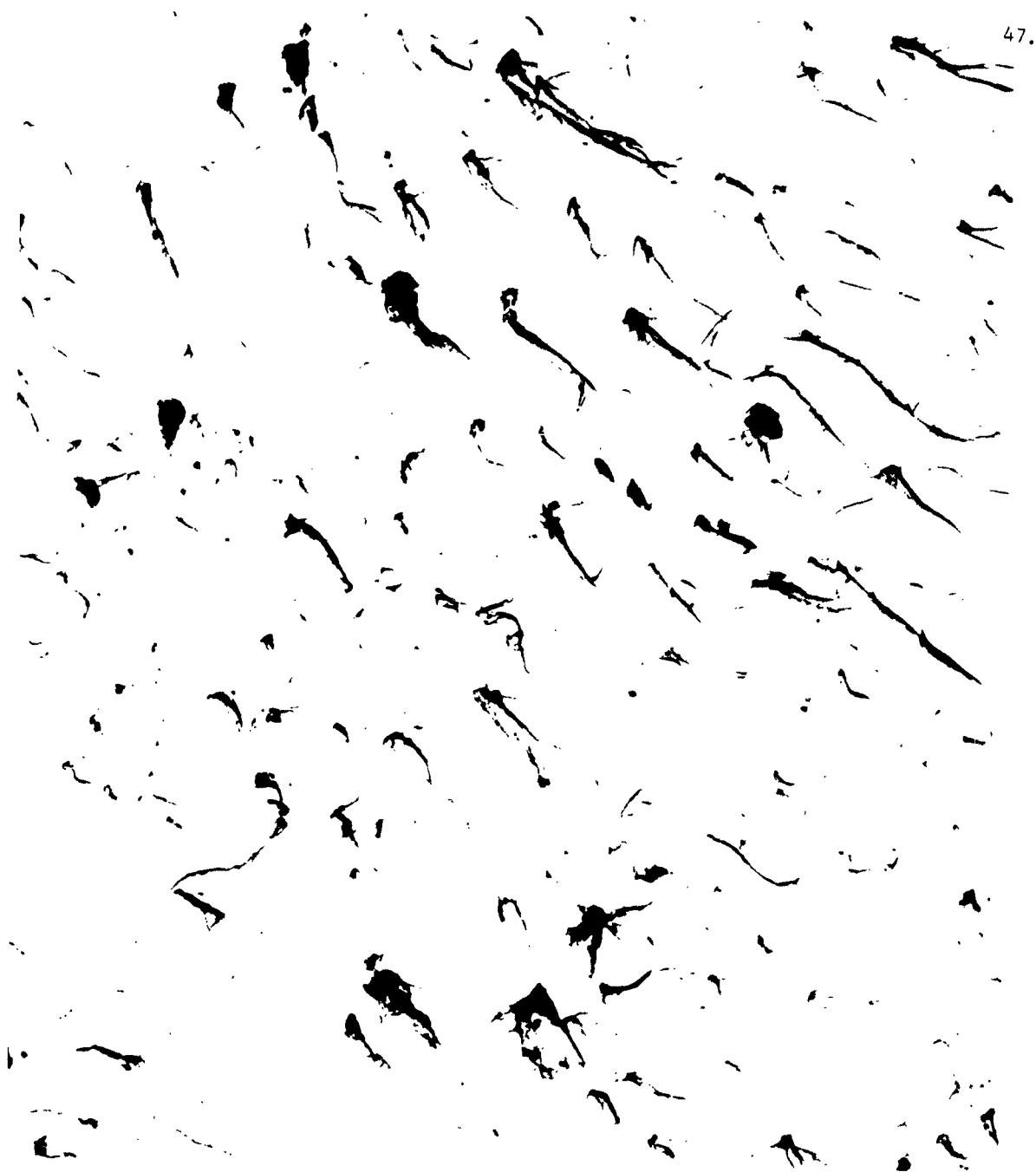
Figure 49. Electron Fractograph of Fracture Surfaces in the Weld (120 inch
Maraging Steel Vessel Closure Plate) Dark Appearing Particles are
Probably Titanium Carbides or Nitrides
12,000X   Carbon Replica
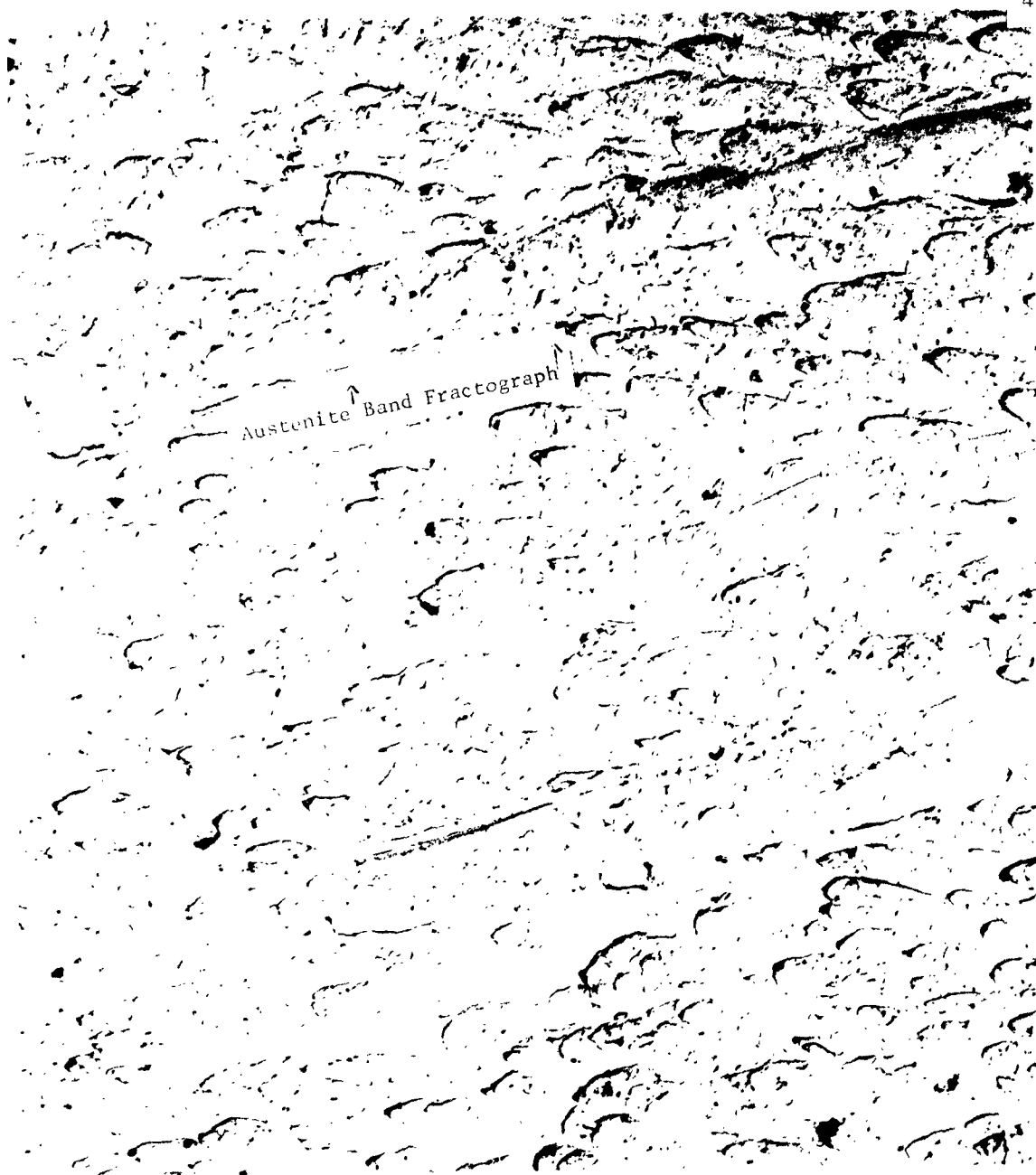
Figure 50. Electron Fractograph of Fracture Surfaces in Banded Area of 5/8 inch
Thick Plate (120 inch Maraging Steel Vessel Closure Plate)
7,000X   Carbon Replica
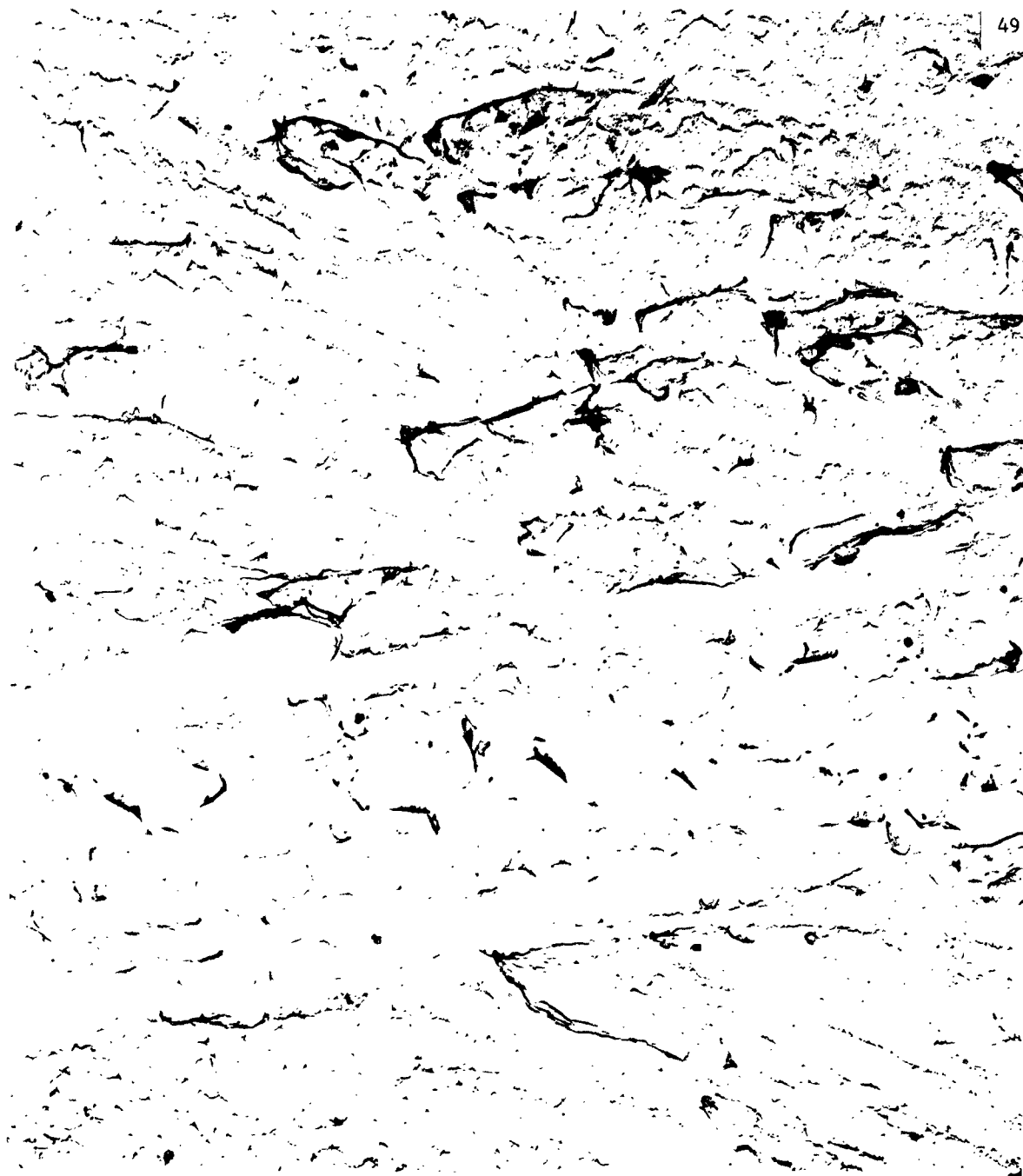
Figure 51. Electron Fractograph of Specimen of Figure 50 at Higher Magnification Showing Positioning of Carbides, Inclusions, etc., Along the Austenite Band

24,000X   Carbon Replica

Kinked Austenite Band
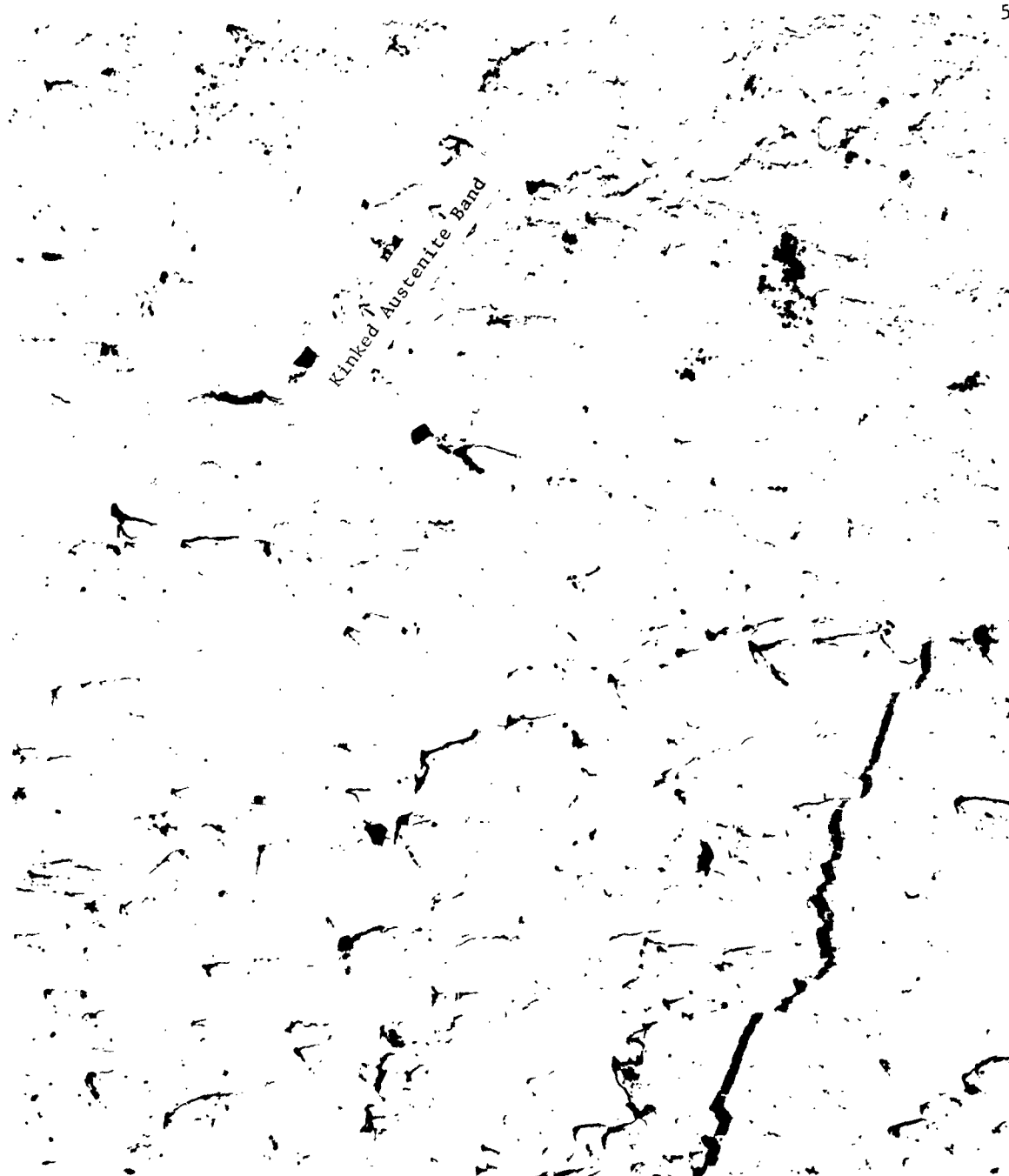
Figure 52. Electron Fractograph of Fracture Surface in 5/8 inch Maraging
18Ni Steel Plate Showing Deformation Markings Leading to Kinking
in Austenite and Development of Micro-cracks
7,000X   Carbon Replica
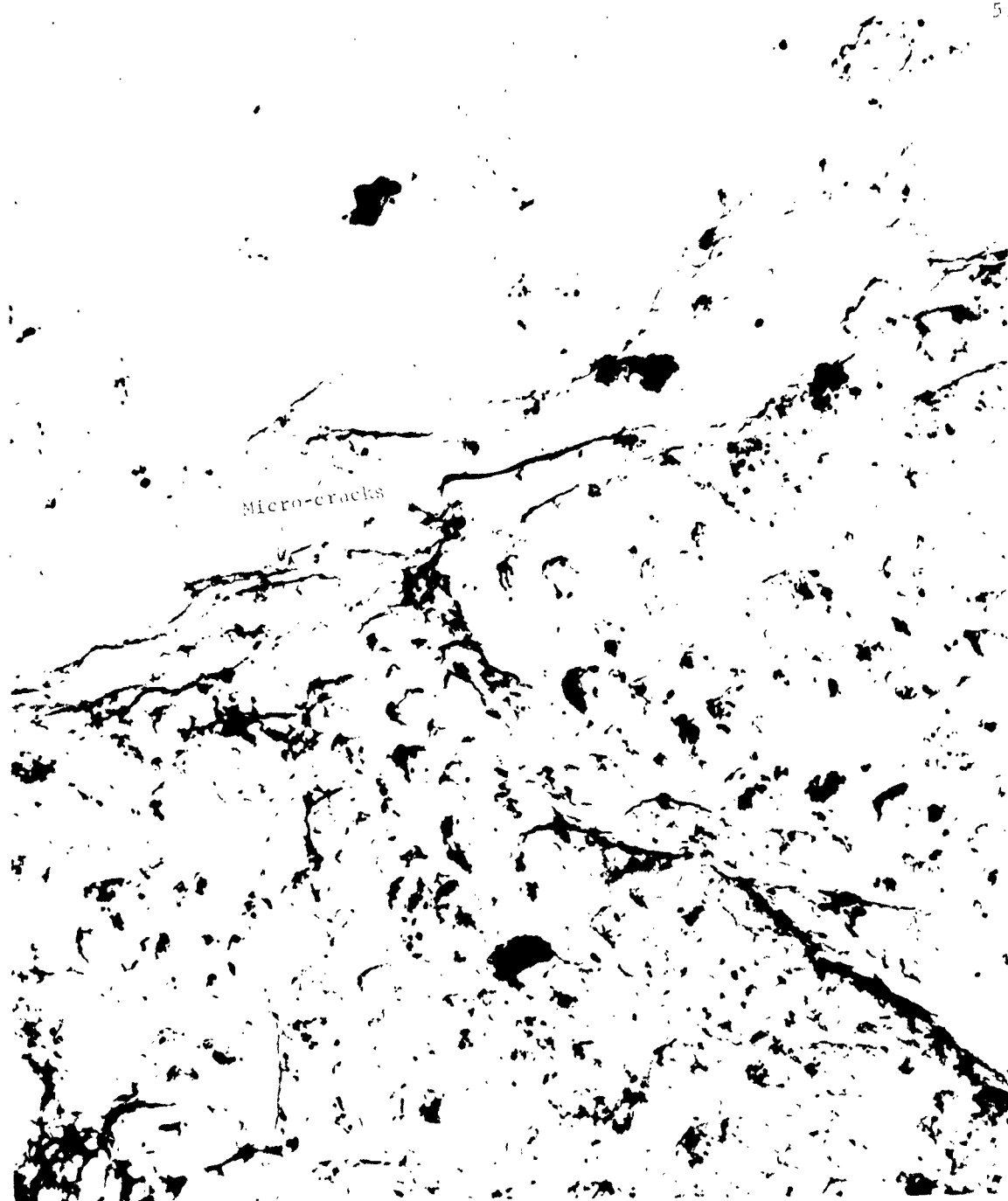
Micro-cracks

Figure 53.   Electron Fractograph of Fracture Surface at 5/8 inch Maraging 18Ni
Steel Plate - Weld Interface Showing Austenite Deformation and Micro-
Crack Formation
7,000X   Carbon Replica
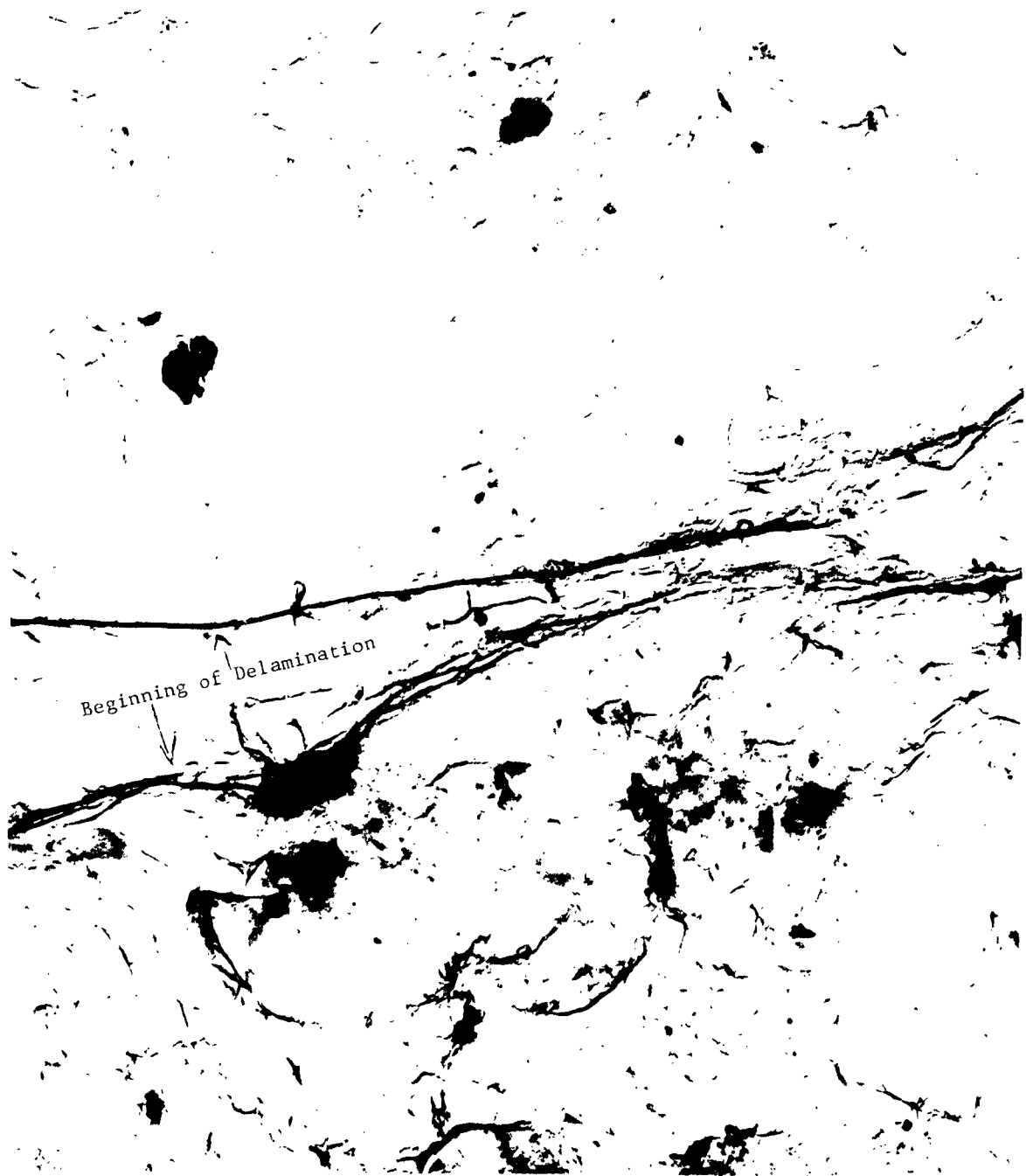
Figure 54. Electron Fractograph of Fracture Surfaces in Same Specimen, as in
Figure 53, but Different Locations - Showing Separation Leading
to Delamination at Plate-Weld Interface
7,000X   Carbon Replica
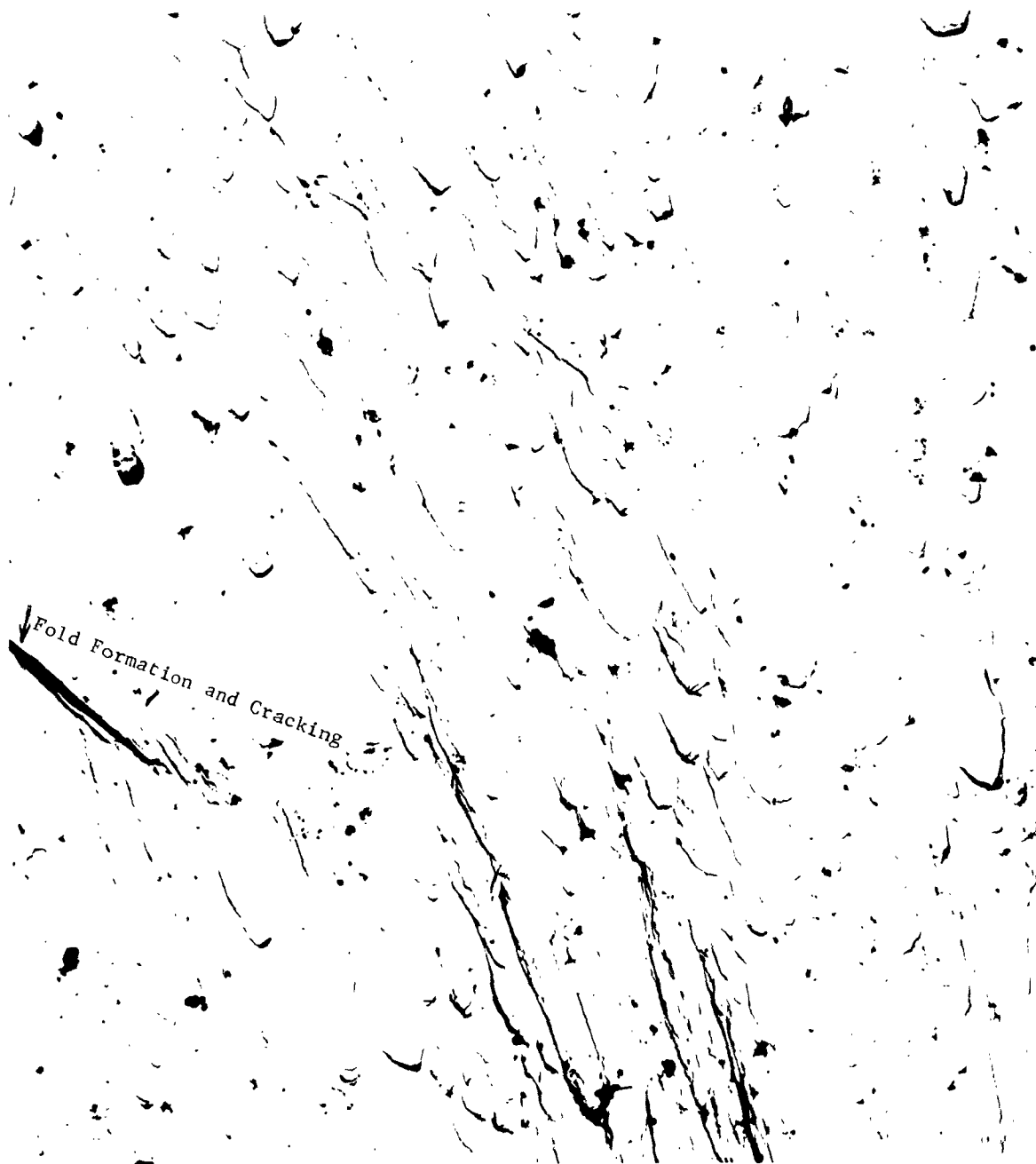
Figure 55. Electron Fractograph of Fracture Surfaces in 5/8 inch Maraging 18Ni
Steel Plate of 120 inch Vessel Closure Plate, Depicting Interplanar
Shear Leading to Formation of Folds and Cracks in the Fold
7,000X   Formvar Replica

MECHANICAL PROPERTY EVALUATION OF CLOSURE PLATE MATERIALS

In this phase, attempts vere made to associate the premature fracture of the closure plate with any mechanical strength deficiency which may have existed in the components of the closure plate. Accordingly, tensile test and Charpy impact test specimens were extracted from several locations as indicated in Figure 56. Specimen cutting was done through the use of a plasma arc cutting torch. The burnt edges of these specimens were ground off prior to machining of the required specimens.

Mechanical Properties of Plate Material
Tensile Strength of 5/8 inch Thick Plate

| Specimen Identification	1	2	3
Yield Strength 0.2% Offset, KSI	256	249	248
Tensile Strength, KSI	269	258	257
Fracture Stress, KSI	308	327	347
% Reduction in Area	36	41	45
% Elongation in 1 inch	(a)	22	22
% Elongation in 2 inches	(a)	11.5	11.5

(a) - Specimen broke outside 2 inch gage mark showing delamination slits which did not appear until average yielding occurred.

Slow Bend Fracture Strength of 5/8-inch Thick Plate

Specimen Identification	Notch Location Surface	Crack Depth in.	Break Loads lbs.	G_c Psi-in.
5	Surface	0.110	4860	685
6	Side	0.112	3490	342
7	Surface	0.108	6050	1030
8	Side	0.113	3590	380

TENSILE SPECIMEN: 0.375" ± 0.030" THICK
BEND BARS : LENGTH = 8.000" ± .125"
WIDTH = THICKNESS = .625" ± .005"
NOTCH DEPTH = 0.094" ± 0.005"
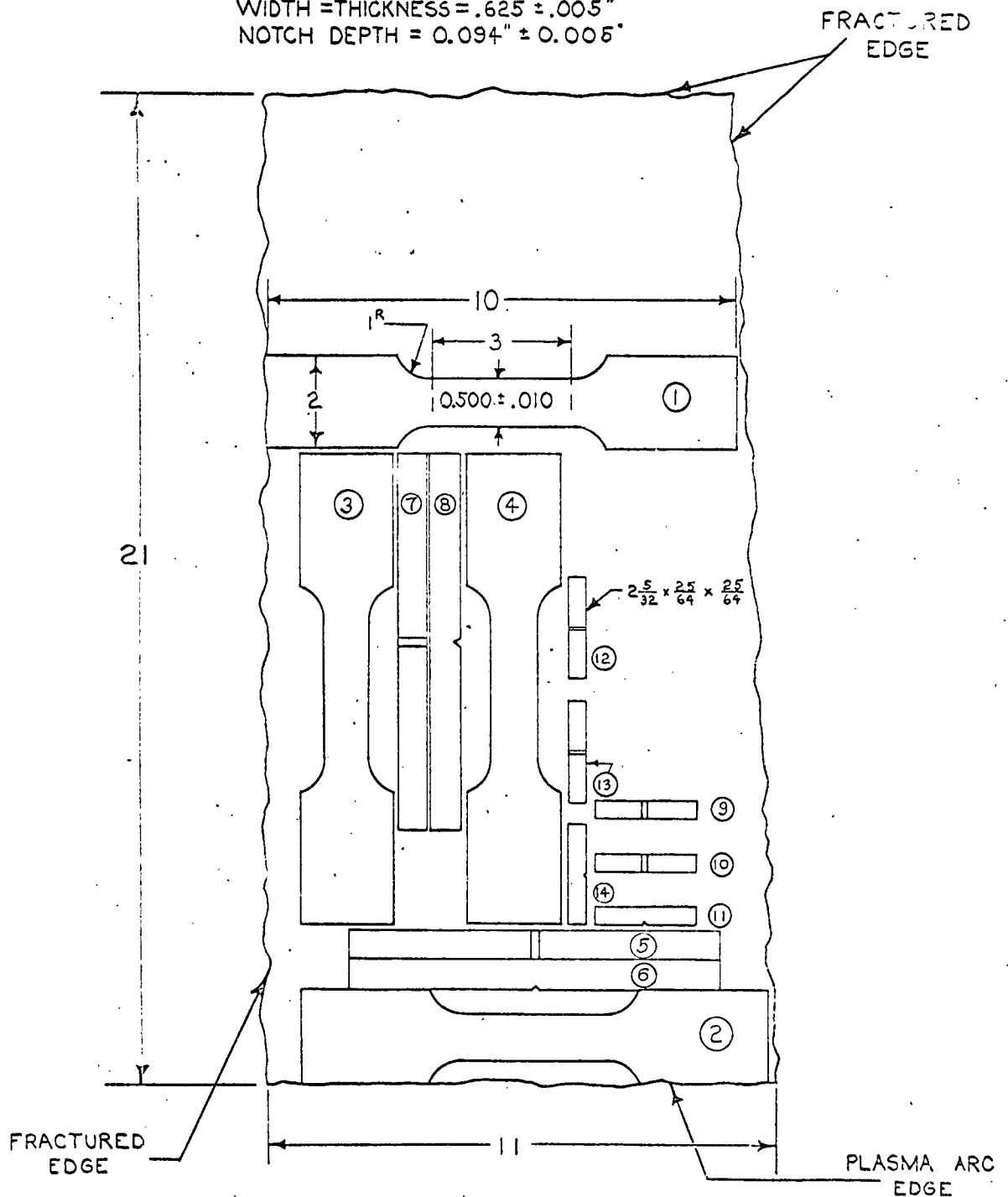
Figure 56. Mechanical Test Specimen Extraction Plan for 5/8" Plate

REVISION		SAMPLING : FOR 120 CLOSURE PLATE		
REF. DWGS.				
		DATE 10/30/63	DRAWN L. MASSUNG	CHARGE NO.
DWG. NO.		SCALE ¼ SIZE	CHECKED	APPROVED

Charpy Impact Strength of 5/8-inch Thick Plate

Specimen Identification	Notch Location	Energy Absorbed ft. lbs.	Specimen Location
9	Surface	12.0	CD
10	Surface	13.0	CD
11	Side	13.0	CD
12	Surface	18.5	AD
13	Surface	17.0	AD
14	Side	15.5	AD

CD - Close to delaminated area
AD - Away from delaminated area

Mechanical Properties of Material from Ring Forging
Tensile Strength

Two flat tensile specimens, approximately 0.380 inches thick were

plasma arc cut from locations as indicated in Figure 57, machined to dimen-

sions and tested. The results obtained are as follows:

Specimen Identification	P2	P3
Yield Strength 0.2% Offset, KSI	231	228
Tensile Strength	232	236
% Reduction in Area	24	26
% Elongation in 1 inch	(a)	(a)
% Elongation in 2 inches	(a)	6

(a) Specimens broke outside respective gage marks

Fracture Toughness

Part-Through Fatigue Cracked Specimen (1½"W x 18"L x 0.4"T)

Specimen No.	Plate Thickness in.	Crack Depth in.	Crack Length in.	Crack "Pop-in" Load, lbs.	"Pop-in" Stress KSI	K_{Ic} Ksi√in.
P1	0.418	0.177	0.90	80,600	126	91.8

P2 & P3 TWO FLAT
SPECIMENS 10 × 1 × 2½

P1 - PART THRU CRACK
SPECIMEN 18 × 2½ × 1
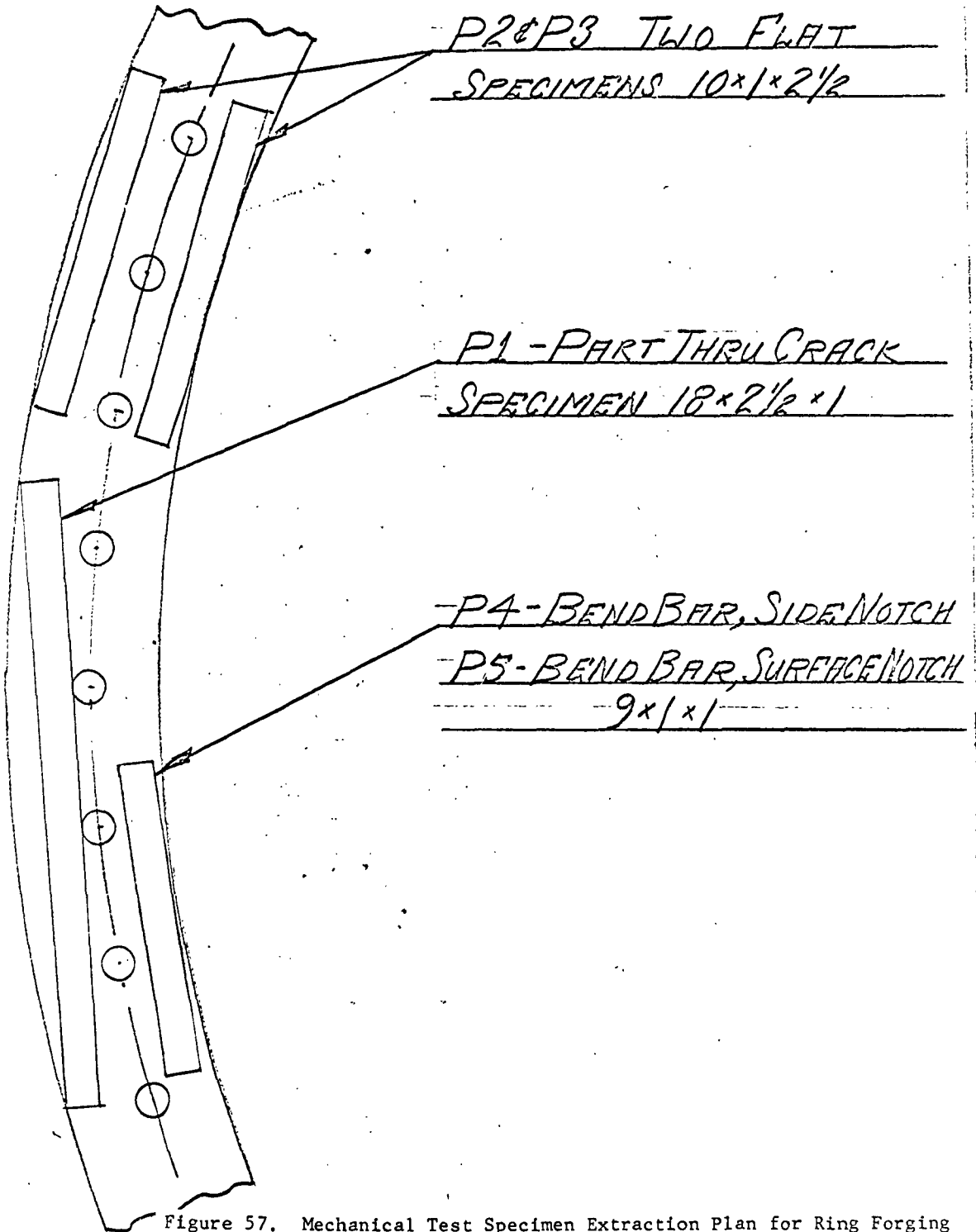
-P4 - BEND BAR, SIDE NOTCH
P5 - BEND BAR, SURFACE NOTCH
9 × 1 × 1

Figure 57. Mechanical Test Specimen Extraction Plan for Ring Forging

MELLON INSTITUTE, PITTSBURGH, PA.

120" CLOSURE FORGING

REVISION		
REF. DWGS.	DATE 10/28/63	DRAWN
DWG. NO.	SCALE NONE	CHECKED

Slow Bend Fracture Tests (5/8" Square Specimens)

Specimen Identification	Notch Location	Crack Depth in.	Break Load lbs.	G_c psi-in.	Specimen Location
P4	Internal Side	0.116	2370	164	Thick Section
P5	External Surface	0.120	3540	374	Thick Section

Mechanical Properties of Ring Forging Material
Heat Treated Separately at Mellon Institute

Round Tensile Specimens (0.350 inch diameter)

Specimen No.	1	2	3
Yield Stress, KSI 0.2% Offset	247	257	259
Tensile Stress, KSI	258	265	266
Fracture Stress, KSI	338	326	332
% Reduction in Area	50	45	47
% Elongation in 1 inch	18	12	16

Mechanical Properties of Bolt Material

Tensile Properties (Unnotched (smooth) bars)

Specimen No.	1	2	3
Specimen Diameter, inches	0.248	0.500	0.500
Yield Strength, KSI 0.2% Offset	250	270	271
Tensile Strength, KSI	258	278	281
Fracture Strength, KSI	285	351	357
% Reduction in Area	31	46.9	47.4
% Elongation in 1 inch	2.5	19	18

Notched Tensile Properties [a] (0.500 inch diameter bars)

Specimen No.	1	2
Notched Bar Diameter, inches	0.404	0.402
Notched Section Stress	320	327

(a) The notched specimens actually yielded prior to break, thus showing excellent notch toughness

Two full section notched tensile bars having two threads of same dimensions, as in the bolts were machined, maraged at 915F for 4 hours and subsequently tested. In three trials, one of the specimens was loaded to a net section stress of 292 KSI when the specimen grip threads stripped off. These tests had to be discontinued since additional grip costs became excessive.

Since the threads in all 68 bolts had been machine cut, the root radius in the threads of all bolts were carefully checked. Stress concentration factor K_t of all except one bolt thread ranged from $K_t=3$ to $K_t=4.5$. In the one exception, a thread K_t of 6.3 had been noticed. The hardness of bolts varied in the narrow range Rockwell C 50.5 to 51.9, indicating good control of aging treatment.

Hardness transverse taken through a cross-section representing the forging, weld and the plate indicated that the hardness varied from Rockwell C 48 in the forging, R_c50 in the weld, $R_c51.8$ in the heat affected zones to R_c in the 5/8 inch plate.

Mechanical Properties of Ring Forging to Parent Plate Weld Transition Area

Only Charpy impact properties of ring forging to 5/8 inch thick plate weld transition area were studied. Notches were located on the surface as well as on the thickness side of the forging and also the plate. The Charpy impact strength data thus obtained are as tabulated:

Specimen No.	Material	Notch Location	Charpy Impact Strength ft. lbs.
1	Forging	Surface	10.0
2	Forging-Weld, Fusion Zone	Surface	11.5
3	Forging	Side	10.0
4	Forging-Weld, HAZ	Side	11.5
5	Weld	Surface	24.0
6	Weld-Plate, Fusion Zone	Surface	21.5
7	Weld-Plate, HAZ	Surface	16.5
8	Plate	Surface	20.5
9	Plate	Surface	17.0
10	Plate	Side	10.0
11	Plate	Side	11.0

FRACTURES IN MECHANICAL TEST SPECIMENS

Severe delaminated condition seen in broken tension test specimens taken from the 5/8 inch thick plate has been shown in Figure 58. In contrast, the clean fracture surfaces seen in the broken K_{Ic} test specimen representing the forging is depicted in Figure 59. The grain size of the forging displayed in Figure 60, is judged to be ASTM 4 and smaller.

Tension markings seen in 13 of the 68 bolts can be discerned from Figure 61. From this, it can be inferred that some of these bolts may have failed because of a lack of strength, or because of imposition of combined shear and bending loads beyond the strength capability of these bolts. The strength limiting factors include lack of adequate fracture toughness at 300 KSI strength level (notch brittleness), stress corrosion, hydrogen embrittlement (because of moist environment), etc. Of these, the former two factors were cursorily explored. The later factor was assumed least effective from data of Troiano, and therefore, was not further studied in this program.

Fracture surfaces seen in bolts which failed under predominately shear loading conditions are shown in Figure 62.

Fracture surfaces displayed by the broken Charpy Impact test specimens from the forging to plate weld transion area are shown in Figure 63. It will be clearly noticed that the ring forging specimens do not exhibit the splits seen in the fracture surfaces of plate specimens.

Figure 58.   Severe Delaminations Seen in Broken 5/8 inch Plate Tension Test Specimens (120 inch Vessel Closure Plate)

Figure 59.   Clean Fracture Surfaces Seen in K_{Ic} Fracture Test Specimens Extracted from the Ring Forging. (120 inch Vessel Closure Plate)
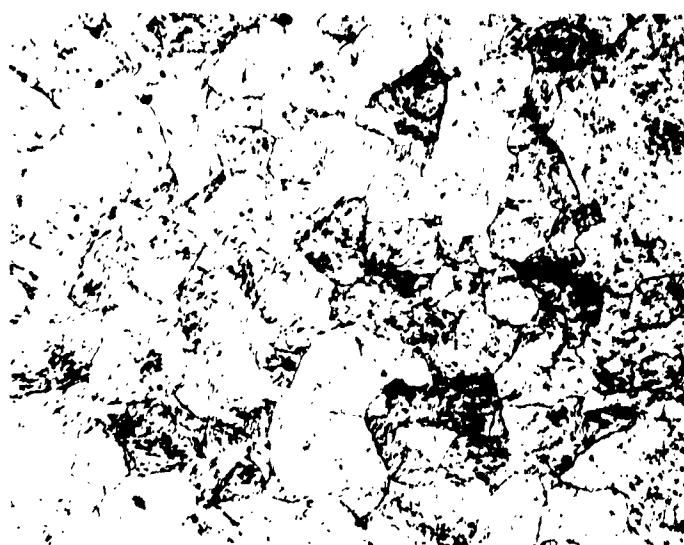
MELLON INSTITUTE

Figure 60. Grain Size of Ring Forging Used in 120 inch Vessel Closure Plate
ASTM 4.

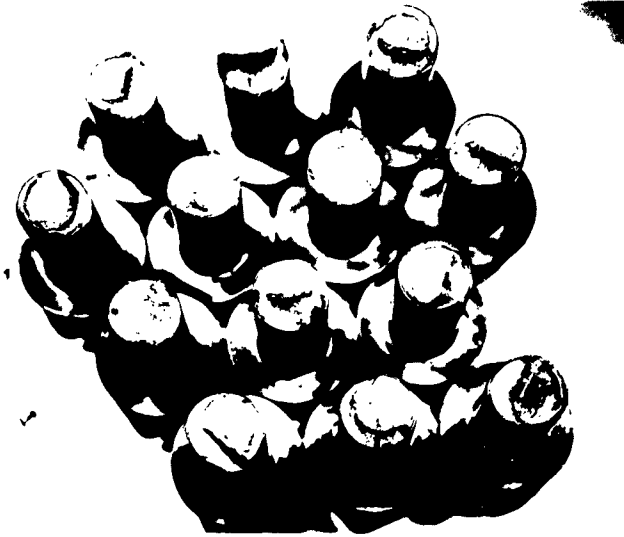Chloride Etch   100X

Figure 61. Tension Marking Seen in 13 Bolts Close to Plate Delamination Origin Area. (120 inch Vessel Closure Plate)

Figure 62. Typical Shear Markings Seen in 55 Bolts which Held the 120 inch Vessel Closure Plate Attached to the Vessel During Hydrotest.

Fracture Surface in Leg

Fracture in
Ring Side of
Weld

Fractures in Plate
Side of Weld

Fractures in Plate

Figure 63.   Fractures Seen in Impact Test Specimens Extracted from a
Ring-to-Plate Weld Section.

DISCUSSION

Metallographic evidence presented of the deformation of banded areas in the 5/8 inch plate of the closure plate while the membrane stresses in the closure plate were around 105,000 psi is strong enough to conclude that de-lamination of the plate could have been the primary cause of closure plate failure. On the other hand, the loss of shear lip points out yet another cause of closure plate separation. From a metallurgical structural view point, little can be said about the later indication. The forging material had no apparent defects which affected its performance. Therefore, except for this mention of the second probable cause, this matter will be left to the designer for further evaluation.

The 5/8 inch thick plate had obvious defects which were manifested in the peculiar fracture markings and loss of short transverse (through-the thickness) mechanical strength. The later has been confirmed through the bend fracture toughness and impact strength studies.

The bolt failure cannot be related to any specific material defi-ciencies. Conversely, it is doubted that any of the bolts actually failed prior to achieving their designed strength (280 KSI) level. Stress corrosion tested bolts (full section), 100 hour exposure in water and torqued to 600 lbs., 1,000 lbs., and 1,250 lbs. did not fail when stressed to 268 KSI. The tensile test machine grips were not strong enough to test these bolts beyond this stress level. These tests were incomplete; however, the results indicated that stress corrosion was not a factor in this case.

It is also clear from the deformation markings seen in banded micro-structures that the plate did not delaminate due to impact with the I beam.

Some secondary fractures may have occurred as a result of this impact. But because the fracture markings in the forging showed evidence of "bending out" this can be used as further evidence to conclude that the delamination occurred almost through centrally in the plate which then opened out during internal pressurization as two hinged doors.

Defects seen in the weld can be attributed largely to the banded condition of the plate and suction of these defects during weld solidification into the weld puddle, fusion zone and the heat affected zone. Maraging 18Ni (250 KSI) plates which are free of segregation have never been known to crack during welding by TIG method. Therefore, transverse cracking in banded plates cannot be considered as a problem created by a qualified fabricator. Rather, the material deficiency leads to the degradation of weld strength and questionable performance of the finish fabricated motor case.

It is to be understood that the writer has attempted to draw conclusions only from overwhelming evidence and not from chance occurrence or hidden meanings to be attached to the physical evidence of the closure plate fracture or the data developed in this program.

CONCLUSIONS

1. The metallurgical data developed through an analyses of the failed closure plate of the 120 inch maraging 18Ni (250 KSI) steel vessel, has indicated that plate delamination might have been the primary cause leading to the component fracture, prior to achieving the designed strength level.

2. Presence of large amounts of austenite and segregation of carbide and other inclusions in banded areas leads to delamination of the plate. The delamination starts from a large interplanar crack or

series of interplanar micro-cracks which seem to develop in the bands either due to austenite transformation stresses when heat, as in welding or cutting, is applied at the location of bands or due to deformation and kinking of the austenite in the bands when the plate is stressed beyond the yield strength of the austenite. It is to be pointed out that the austenite present in the band yields much earlier than the aged martensitic structure of the 18 per cent nickel steel plate.

3. The separation of 70 per cent of the shear lip in the forging also points out some design deficiency. To what extent this has contributed to the premature failure of the closure plate has been left to the designer for a decision. From a metallurgical standpoint, the forging had no apparent defects and it had adequate mechanical strength including fracture toughness.

4. Despite these problems, which have to be alleviated or eliminated, the maraging 18 per cent nickel 250 KSI steel still appears to be the best candidate material for application in big booster. The delamination problem is receiving urgent attention from the steel producers.